haematologica
Journal of the Ferrata Storti Foundation

Small extracellular vesicles derived from acute myeloid leukemia cells promote leukemogenesis by transferring miR-221-3p

by Mengyu Li, Guohuan Sun, Jinlian Zhao, Shuangshuang Pu, Yanling Lv, Yifei Wang, Yapu Li, Xiangnan Zhao, Yajie Wang, Shangda Yang, Tao Cheng, and Hui Cheng

Received: August 24, 2023.
Accepted: February 29, 2024.

Citation: Mengyu Li, Guohuan Sun, Jinlian Zhao, Shuangshuang Pu, Yanling Lv, Yifei Wang, Yapu Li, Xiangnan Zhao, Yajie Wang, Shangda Yang, Tao Cheng, and Hui Cheng. Small extracellular vesicles derived from acute myeloid leukemia cells promote leukemogenesis by transferring miR-221-3p. Haematologica. 2024 Mar 7. doi: 10.3324/haematol.2023.284145 [Epub ahead of print]

Small extracellular vesicles derived from acute myeloid leukemia cells promote leukemogenesis by transferring miR-221-3p

Mengyu Li[1,2#], Guohuan Sun[2,3,4#,] Jinlian Zhao[5#], Shuangshuang Pu[2,3,4], Yanling Lv[2], Yifei Wang[2], Yapu Li[2,3,4], Xiangnan Zhao[2,3,4], Yajie Wang[5*], Shangda Yang[2,3,4*], Tao Cheng[1,2,3,4*] and Hui Cheng[2,3,4*]

[1]State Key Laboratory of Experimental Hematology; The Province and Ministry Co-sponsored Collaborative Innovation Center for Medical Epigenetics, Key Laboratory of Immune Microenvironment and Disease (Ministry of Education), Department of Cell Biology, School of Basic Medical Sciences, Tianjin Medical University, Tianjin, China.

[2]State Key Laboratory of Experimental Hematology, National Clinical Research Center for Blood Diseases, Haihe Laboratory of Cell Ecosystem, Institute of Hematology & Blood Diseases Hospital, Chinese Academy of Medical Sciences and Peking Union Medical College, Tianjin, China.

[3]CAMS Center for Stem Cell Medicine, PUMC Department of Stem Cell and Regenerative Medicine, Tianjin, China.

[4]Department of Stem Cell & Regenerative Medicine, Peking Union Medical College, Tianjin, China.

[5]Department of Hematology, National Key Clinical Specialty of Hematology, Yunnan Blood Disease Clinical Medical Center, Yunnan Blood Disease Hospital, The First People's Hospital of Yunnan Province, Kunming, China.

#These authors contributed equally.

*Correspondence: chenghui@ihcams.ac.cn (HC), chengtao@ihcams.ac.cn (TC), yangshangda@ihcams.ac.cn (SDY) and kbb165wyj@sina.com (YJW).

Keywords: Acute myeloid leukemia; Small extracellular vesicles; miR-221-3p; *Gbp2.*

Disclosures

No conflicts of interest to disclose.

Author contributions

MYL, GHS, and JLZ designed the study and performed the experiments. YLL helped with the bioinformatics analyses. SSP, YFW, YPL and XNZ helped with the mouse experiments. YJW, SDY, TC, and HC conceptualized the study, designed the experiments, interpreted the results, wrote the paper, and oversaw the study.

Funding

This work was supported by grants from the Ministry of Science and Technology of China (2021YFA1100900, 2020YFE0203000), the National Natural Science Foundation of China (81890990, 82270120 ,82070173), the Haihe Laboratory of Cell Ecosystem Innovation Fund (22HHXBSS00016), the CAMS Initiative for Innovative Medicine (2021-I2M-1–019 and 2021-I2M-1–040), the CAMS Fundamental Research Funds for Central Research Institutes (3332021093), Basic Research Special Program for Talented Youths of Yunnan Province (202101AW070017) and The Yunnan Province Thousand Talents Plan (KH-SQR-2020).

Data-sharing statement

All data are available upon request sent to the corresponding author.

Acknowledgments

We are grateful to any members of our laboratory not listed in the author section for their assistance with the experiments performed during this study.

Abstract

Small extracellular vesicles (sEVs) transfer cargos between cells and participate in various physiological and pathological processes through their autocrine and paracrine effects. However, the pathological mechanisms employed by sEV-encapsulated microRNAs (miRNAs) in acute myeloid leukemia (AML) are still obscure. In this study, we aimed to investigate the effects of AML cells-derived sEVs (AML-sEVs) on AML cells and delineate the underlying mechanisms. We initially used high-throughput sequencing to identify miR-221-3p as the miRNA prominently enriched in AML-sEVs. Our findings revealed that miR-221-3p promoted AML cell proliferation and leukemogenesis by accelerating cell cycle entry and inhibiting apoptosis. Furthermore, *Gbp2* was confirmed as a target gene of miR-221-3p by dual luciferase reporter assays and rescue experiments. Additionally, AML-sEVs impaired the clonogenicity, particularly the erythroid differentiation ability, of hematopoietic stem and progenitor cells. Taken together, our findings reveal how sEVs-delivered miRNAs contribute to AML pathogenesis, which can be exploited as a potential therapeutic target to attenuate AML progression.

Introduction

Acute myeloid leukemia (AML) is a malignant blood disease characterized by abnormal growth and differentiation of hematopoietic stem/progenitor cells (HSPCs). The leukemic cells infiltrate the bone marrow (BM), peripheral blood, and extramedullary tissue, leading to cytopenia and death.[1-3] The BM is composed of hematopoietic and non-hematopoietic cells, which participate in multiple biological processes together with the extracellular matrix.[4] Under physiological conditions, the BM plays a critical role in supporting and regulating the self-renewal, multi-lineage differentiation, apoptosis, resting, and trafficking of HSPCs.[5] Leukemic cells remodel the BM microenvironment into a leukemia-permissive one, impeding residual HSPCs function and contributing to leukemia progression.[6] However, the mechanisms by which BM cells create and maintain the leukemic BM niche, as well as how this leukemic niche subsequently impacts leukemic cells and HSPCs, remain to be explored.

The leukemic BM niche is intricate for extensive cell-cell interactions and biological processes, which are regulated by extracellular components such as cytokines, chemokines, and extracellular vesicles.[7,8] For instance, leukemic cells interact directly with mesenchymal stromal cells to inhibit normal hematopoiesis and promote leukemic cell proliferation through the secretion of CCL3 and THPO.[9] Moreover, leukemic cells upregulate the expression of *CXCR4* and *VLA4*, leading to drug resistance.[10] Our previous research also demonstrate that the CCL3 secreted by leukemic cells inhibits erythropoiesis,[11] while BM endothelial cells inhibit the differentiation and maturation of megakaryocytes by expressing high level of interleukin (IL)-4 in MLL-AF9

mouse model.[12] By contrast to traditional forms of intercellular communication, extracellular vesicles (EVs) act as messengers by transferring their contents to recipient cells. Small EVs (sEVs) have a 30-150 nm diameter and play pivotal roles in cellular communication by transporting cargos such as nucleic acids, proteins, and lipids, between cells. Accumulating studies have demonstrated that sEVs participate in various physiological and pathological processes by transferring cargos to adjacent or distant cells through paracrine or endocrine pathways, as well as acting on the same cell population through an autocrine effect.[13,14] Importantly, studies have shown that sEVs derived from AML cells (AML-sEVs) can transmit cargos to stromal cells and HSPCs, thereby affecting their functions and, in turn, impacting leukemia progression.[8]

MicroRNAs (miRNAs) are a class of non-coding RNAs, 20-24 nucleotides in length, typically bind to the 3' untranslated regions (3'UTR) of messenger RNAs (mRNAs) to regulate gene expression at the post-transcriptional level.[15] The miRNAs contained in sEVs have been extensively explored because of their abundance, diversity, and ability to regulate mRNA function. Emerging studies have confirmed that sEVs-miRNAs play a vital role in the occurrence, development, diagnosis, and treatment of various tumors.[16,17] However, the specific roles of sEVs-miRNAs in AML and the repertoire of miRNAs within AML-sEVs remain largely unknown. Therefore, the aims of the present study were to identify the miRNAs prominently expressed in AML-sEVs and explore the functions and molecular mechanisms of critical miRNAs in AML development as well as normal hematopoiesis.

Methods

Mice and transplantation

C57BL/6J and B6.SJL mice were purchased from the animal facility of the State Key Laboratory of Experimental Hematology (SKLEH, Tianjin, China). All animal procedures were performed in compliance with the animal care guidelines approved by the Institutional Animal Care and Use Committees of the SKLEH and the Institute of Hematology. To establish the AML model, lineage$^-$ cells were isolated from B6.SJL mouse (CD45.1$^+$) bone marrow and transduced with a retrovirus expressing MLL-AF9 fusion gene.[18] After 72 hours, the cells were injected into lethally irradiated (9.5 Gy) C57BL/6J recipient mice (CD45.2$^+$) to induce AML development. Primary leukemic cells from bone marrow or spleen were harvested and transplanted into non-irradiated recipients (CD45.2$^+$) to establish MLL-AF9 AML model. For MLL-AF9 mouse model, 1×10^5 AML cells were intravenously injected into 6–8-week-old wild-type (WT) C57BL/6 recipient mice. For AML1-ETO9a mouse model, 1×10^5 established AML cells (A gift from Dr. Jianxiang Wang, Chinese Academy of Medical Sciences and Peking Union Medical College) were intravenously injected into 6–8-week-old WT C57BL/6 recipient mice after 5 Gy irradiation. For sEVs in vivo treatment, 40 μg sEVs was injected intravenously or 20 μg sEVs was injected into one tibia of C57BL/6 mice.

Flow cytometry

Apoptosis of AML cells was measured by labeling the cells with Annexin-V-APC for 15 min in 1× binding buffer, according to the manufacturer's instructions (BD Bioscience). For Ki67 staining, AML cells were first fixed and permeabilized

using the Intrasure Kit (BD Bioscience) and then stained with Ki67-APC antibody (BD Bioscience) for 30 min. For $cKit^+$ cells sorting, antibodies (all purchased from BD Bioscience) targeting the following molecules were used: CD3, CD4, CD8, B220, Gr-1, Mac-1, Ter-119, Sca1, cKit. For erythroid differentiation analysis, Ter-119 antibody was used. For the leukemic granulocyte macrophage progenitors (L-GMPs) analysis, antibodies (all purchased from BD Bioscience) targeting the following molecules were used: CD3, CD4, CD8, B220, Gr-1, Ter-119, Sca1, cKit, CD34, CD16/32 (FcγR), CD127 (IL-7Rα), and CD45.1. An anti-CD45.1 antibody (BD Bioscience) was used in the analysis of peripheral blood cells. Finally, 4′,6 diamidino-2-phenylindole (DAPI, Sigma-Aldrich) was added to exclude the dead cells prior to analysis. The analysis was conducted using a BD LSRFortessa flow cytometer, and cell sorting was performed using a BD FACSAriaIII flow cytometer.

Statistical analysis

All experiments were repeated a minimum of three times. The data were analyzed using TreeStar FlowJo software. Quantitative values were presented as means ± standard deviation (SD). The unpaired, two-tailed Student's t-test was used to compare two groups. The one-way ANOVA with Tukey's multiple comparison post-test or a two-way ANOVA with Sidak's multiple comparison test was used to compare more than two groups. Statistical analysis was performed using GraphPad Prism 9.0 and statistical significance was denoted by asterisks (*p<0.05, **p<0.01, ***p<0.001), whereby p-values less than 0.05 were considered as a measure of statistical significance.

Results

AML-sEVs promote AML cell growth through autocrine effects

Previous studies have shown that sEVs derived from leukemic cells participate in leukemia development.[19] To evaluate the impact of AML-sEVs on the growth of AML cells, we isolated sEVs from the culture supernatant of AML cells, previously isolating from the BM of MLL-AF9 AML mouse, by ultracentrifugation according to established protocol (Figure 1A).[20] The structure of sEVs was assessed using transmission electron microscopy, which revealed that they had a typical saucer-like shape (Supplementary Figure S1A). Moreover, nanoparticle tracking analysis determined that the peak particle diameter ranged from 93 to 242 nm, with a mean diameter of 130 nm (Supplementary Figure S1B). Western blotting also confirmed that the isolated sEVs expressed high level of sEVs-specific protein markers (e.g., CD63, CD9, and TSG101) but exhibited negligible expression of the sEVs exclusion marker Calnexin (Supplementary Figure S1C).

Co-culturing AML cells with the isolated AML-sEVs for 3 days significantly increased their proliferation versus that of untreated AML cells (Supplementary Figure S1D). Treating AML cells with GW4869, an inhibitor of sEV secretion, significantly inhibited AML cell growth and viability *in vitro*. Notably, this inhibitory effect was counteracted by treating the AML cells with AML-sEVs (Figure 1B-C). To assess whether these treated cells affect leukemogenic progression *in vivo*, we transplanted the treated AML cells into non-irradiated mice. We found the survival of mice transplanted with the GW4869-treated AML cells was prolonged compared with that of mice in the untreated group.

Meanwhile, the survival of mice transplanted with AML-sEV-treated AML cells was shorter than that of the mice transplanted with GW4869-treated AML cells (Figure 1D). To determine why AML-sEVs promoted tumor growth, we investigated the effects of GW4869 treatment on the cell cycle and apoptosis of AML cells. The results showed that GW4869 treatment caused cell cycle arrest, whereas AML-sEV treatment restored cell cycle entry (Figure 1E and Supplementary Figure S1E). We also observed an increase in AML cell apoptosis following GW4869 treatment, which was significantly inhibited upon AML-sEV treatment (Figure 1F and Supplementary Figure S1F). Collectively, these results indicate that AML-sEVs promote the growth of AML cells by facilitating cell cycle entry and inhibiting cell apoptosis through their autocrine effects.

AML-sEVs promote AML cell growth by delivering miR-221-3p to AML cells

To screen differentially expressed miRNAs present in AML-sEVs, small RNA sequencing was conducted on the sEVs isolated from the BM of WT mice and MLL-AF9 AML mice. Considering that the BM supernatant of AML mice contains sEVs from various cellular sources, small RNA sequencing was also conducted using cultured AML-sEVs. We identified 79 upregulated miRNAs that were differentially enriched in BM-derived AML-sEVs relative to WT-sEVs. In addition, we obtained 117 upregulated miRNAs between WT mouse BM sEVs and cultured AML-sEVs (Figure 2A). By intersecting the miRNAs upregulated in AML identified by both analyses, we obtained 35 miRNAs that were highly expressed in AML-sEVs, as shown in the heatmap (Figure 2B).

To validate the sequencing results, we detected the expression level of candidate miRNAs by quantitative real-time PCR (qRT-PCR) and identified six highly enriched miRNAs (miR-5099, miR-221, miR-690, miR-5100, miR-181b-5p, and miR-181d-5p) in both AML-sEVs and AML cells (Figure 2C, Supplementary Figure S2A-C and Supplementary Table 1). Among these miRNAs, miR-5099, miR-690, and miR-5100 were not conserved across various species. By contrast, miR-221-3p (hereafter referred to as miR-221) is conserved in various species and was highly expressed in sEVs isolated from the peripheral blood plasma of AML mice or patients compared with control or healthy individuals, suggesting its important role in AML (Figure 2D-E and Supplementary Figure S2D). Next, we investigated the impact of miR-221-containing sEVs on the growth of AML cells. 293T cells were infected with lentiviruses overexpressing either a scrambled control miRNA (Ctrl-miR) or miR-221. We then isolated sEVs from the conditioned medium to obtain Ctrl-sEVs and miR-221-sEVs, respectively. Subsequent qRT-PCR analysis confirmed the effective overexpression of miRNA-221 in both 293T cells and the resulting sEVs (Supplementary Figure S3A-B). Co-culturing AML cells with miR-221-sEVs significantly increased their proliferation (Figure 2F). Moreover, miR-221-sEVs also rescued the proliferation defect in AML cells caused by GW4869 treatment (Supplementary Figure S3C-H). These findings underscore the crucial role of miR-221 in the autocrine effect of AML-sEVs on AML cell growth.

miR-221 facilitates leukemogenesis by promoting AML cell cycle entry and inhibiting apoptosis

To understand how miR-221 affected leukemic cell function, we knocked down miR-221 in AML cells and found that miR-221 depletion inhibited the growth and colony formation ability of AML cells (Figure 3A-B). Moreover, miR-221 knockdown in AML cells significantly delayed the onset of AML and prolonged the survival of recipient mice (Figure 3C-D). Furthermore, the downregulation of miR-221 was associated with AML cell cycle arrest and increase in AML cell apoptosis (Figure 3E-F). These data indicate that miR-221 is important in AML cell proliferation and survival.

To clarify the oncogenic potential of miR-221, AML cells were infected with a miR-221-overexpressing lentivirus. Overexpression of miR-221 promoted the growth and colony formation ability of AML cells, exacerbating leukemogenesis (Figure 4A-B and Supplementary Figure S4A-B). Consistent with earlier findings, miR-221 promoted the cell cycle entry and inhibited the apoptosis of AML cells (Figure 4C-D). Compared with control group, the ratio of spleen or liver to body weight in overexpressed group was higher (Figure 4E and Supplementary Figure S4C-D). Histological examination of the spleen and liver revealed an increased infiltration of leukemic cells in the miR-221-overexpressing group of mice, in comparison with that of the control group (Figure 4F and Supplementary Figure S4E). Remarkably, while miR-221 overexpression impacted the whole leukemic cell population, it did not appear to affect the frequency of phenotypically defined leukemia stem cells (LSCs) and functional defined LSCs determined by limiting dilution analysis (Figure S4F-H). These results implies that miR-221 predominantly impacts the bulk leukemic cell population rather than specifically targeting LSCs.

Given that AML cells can exert their effects on tumor growth through the sEVs-mediated secretion of miR-221, we next investigated whether the expression of miR-221 in sEVs was influenced by the knockdown or overexpression of miR-221 in AML cells. To achieve this, we collected conditioned medium from miR-221-depleted or -overexpressing AML cells after 48 h of culture and isolated sEVs by ultracentrifugation. qRT-PCR revealed that the expression level of miR-221 significantly decreased or increased in miR-221-depleted or -overexpressing AML cells and their corresponding sEVs respectively, relative to that of the control group (Supplementary Figure S5A-D). The attenuated proliferation and increased apoptosis of AML cells caused by miR-221 knockdown were rescued by co-culturing with miR-221-sEVs for 3 days (Supplementary Figure S5E-G). These results further confirm that AML-sEVs promote the proliferation of AML cells via miR-221 transfer.

miR-221 promotes the proliferation of AML1-ETO9a cells and human leukemic cell lines

To further explore the role of miR-221 in primary leukemogenesis, we employed another AML model driven by the AML1-ETO9a fusion.[21] miR-221 was either knocked down or overexpressed in AML1-ETO9a cells, and the transfected cells were subsequently transplanted into recipients. The results elucidated that miR-221 knockdown in AML cells increased apoptosis and prolonged the survival of recipient mice (Figure 5A). Conversely, the overexpression of miR-221 inhibited the apoptosis of AML cells and shortened the survival of recipient mice, thereby exacerbating leukemogenesis (Figure 5B).

Given that the seed sequence of miR-221 is conserved across species (Supplementary Figure S2D), our investigation extended to various human leukemic cells. We explored the role of miR-221 in MLL-AF9 cell lines (THP-1) and other cell lines with diverse gene mutations (HL-60, Kasumi-1, MOLM-13). Leukemia cells were infected with miR-221-knockdown or a control lentivirus followed by cell proliferation analysis. The results revealed that miR-221 knockdown reduced cell proliferation and cell viability, potentially by promoting apoptosis and cell cycle arrest (Figure 5C-F and Supplementary Figure S6A-C). These findings illustrate the pivotal role of miR-221 in diverse leukemic cell types, thereby expanding its relevance in the intricate landscape of leukemia pathogenesis.

miR-221 increases AML cell proliferation by targeting *Gbp2*

The seed sequence of miRNAs recognizes complementary sequences in the 3' UTRs of downstream target genes, leading to translational inhibition.[22,23] To identify the potential target genes of miR-221, we sorted miR-221-depleted and -overexpressed AML cells for transcriptome sequencing. We identified 130 upregulated genes and 93 downregulated genes in the miR-221 knockdown group versus the scramble group. A further 770 upregulated genes and 781 downregulated genes were identified by comparing the miR-221 overexpressing group with the scramble group (Figure 6A).

In most cases, miRNA negatively regulates the expression of its target gene.[24] By overlapping the upregulated genes from the miR-221 knockdown group with the downregulated genes from the miR-221-overexpressing group, we identified

a set of seven genes as potential targets of miR-221: *Gbp2, Mylip, Pcdh7, Angpt1, Tent5a, Ammecr1, Ddx4* (Figure 6A-B and Supplementary Figure S7A-B). Notably, the Geno Ontology (GO) functional enrichment analyses revealed that predicted target genes of miR-221 were enriched in terms related to cell growth and death processes (Supplementary Figure S7C). To further validate the target genes of miR-221, we inserted the 3'UTR sequence of the candidate genes into a dual luciferase reporter gene vector and co-transfected it with miRNA negative control (miR NC) or miR-221 mimic into 293T cells. The activity level of luciferase in the group co-transfected with *Gbp2* 3'UTR and miR-221 mimic was significantly lower than that co-transfected with *Gbp2* 3'UTR and miR NC (Supplementary Figure S7D). Notably, this reduction in luciferase activity was restored when 293T cells were co-transfected with a vector carrying a mutated 3'UTR sequence of *Gbp2*, indicating that miR-221 interacted with *Gpb2* (Figure 6C). Additionally, we observed that the mRNA and protein expression level of *Gbp2 is* significantly higher in miR-221-depleted AML cells than that in control cells, supporting the notion that miR-221 regulated *Gpb2* expression (Figure 6D and Supplementary Figure S7E).

To explore the effect of *Gbp2* on AML cell, AML cells were infected with *Gbp2*-shRNA or control lentiviruses. The results indicated that *Gbp2* knockdown significantly increased the proliferation and reduced the apoptosis of AML cells (Supplementary Figure S7F-H and Supplementary Table 2). To confirm the regulatory role of miR-221, the *Gbp2*-depleted AML cells were infected with miR-221 knockdown or control lentiviruses. The results demonstrated that knockdown of *Gbp2* attenuated the effect of miR-221 knockdown on

proliferation and apoptosis of AML cells (Figure 6E-F). As previous study showed the role of *Gbp2* in modulating cell proliferation through PI3K/AKT pathway,[25] we assessed the protein expression level of AKT, p-AKT, JNK, p-JNK and BAX in *Gbp2*-overexpressed AML cells and control cells. The results revealed that *Gbp2* overexpression led to a decrease in the protein expression level of AKT, p-AKT, JNK and p-JNK, while increased the expression of BAX (Supplementary Figure S7I). Collectively, these results confirmed that miR-221 promoted AML cell proliferation, in part by targeting *Gbp2*, through regulating PI3K/AKT pathway activation.

AML-sEVs impair HSPCs function through a paracrine effect

In addition to exhibiting autocrine effects, sEVs possess the ability to exert paracrine effects by transferring their cargos to neighboring cells.[26] To explore whether AML-sEVs could be delivered to and internalized by HSPCs, AML-sEVs were labeled with PKH67 and co-cultured with HSPCs for 12 h. Subsequently, the GFP^+ sEVs signal was detected in the cytosol of HSPCs using confocal imaging, indicating that AML-sEVs were delivered to HSPCs (Supplementary Figure S8A).

To investigate the impact of AML-sEVs on HSPC function, we co-cultured AML-sEVs with HSPCs for 3 days and conducted colony formation assays (Figure 7A). AML-sEVs significantly compromised the colony forming ability and proliferation of HSPCs *in vitro* (Figure 7B, Supplementary Figure S8B). To investigate the effect of AML-sEVs *in vivo*, we injected AML-sEVs into WT mice, either via the tail vein or intratibially, and then harvested $cKit^+$ HSPCs from

sEV-treated mice for colony formation assays. Consistent with the *in vitro* co-culture results, the colony-forming ability of HSPCs was impaired following sEV treatment (Supplementary Figure S8C). Coincidentally, there was a decrease in the number of BFU-E, suggesting that AML-sEVs preferentially impaired the erythroid differentiation of HSPCs (Figure 7C). To further investigate this phenomenon, we cultured $cKit^+$ cells with AML-sEVs in an erythroid differentiation culture system and assessed their erythroid differentiation ability. The results revealed a significant reduction in the proportion of $Ter119^+$ cells compared to the control group (Supplementary Figure S8D). These findings indicated that AML-sEVs exerted an inhibitory effect on the erythroid differentiation of normal HSPCs.

To ascertain the main target cells of AML-sEVs within the leukemic BM microenvironment, we sorted immunophenotypically-defined HSPCs, mesenchymal stem cells (MSCs), and endothelial cells (ECs) from the BM of WT and AML mice. The qRT-PCR results showed that miR-221 exhibited the highest fold change in HSPCs, compared with that in MSCs and ECs (Supplementary Figure S8E), indicating that miR-221 may be preferentially transferred to HSPCs. Moreover, co-culturing HSPCs with miR-221-sEVs markedly inhibited their proliferation (Figure 7D). Among the distinct HSPCs compartments, miR-221 displayed the most significant increase in expression fold change in the megakaryocytic-erythroid progenitors (MEPs) and megakaryocyte progenitors (MkPs) of AML mice versus control mice (Figure 7E and Supplementary Figure S8F). To investigate whether the transfer of miR-221 contributes to the AML-sEVs-mediated regulation of HSPCs, we conducted

miR-221 knockdown (KD) in AML cells and collected conditional medium to isolate control- or miR-221KD-sEVs. Subsequently, recipients were intratibially injected with either control- or miR-221KD-sEVs. After 24 h, $Lin^{-}cKit^{+}$ cells were sorted from the tibia and cultured in complete methylcellulose-based medium for 7-10 days. The results indicated that miR-221-contained sEVs mainly affect the BFU-E formation of HSPCs (Figure 7F). Taken together, these data indicate that AML-sEVs preferentially affect the clonogenicity of HSPCs via the transfer of miR-221, thus perturbing their erythroid differentiation ability.

Discussion

Evidence suggests that tumor-derived sEVs contribute to tumor progression, metastasis and therapeutic resistance.[27] In the present study, we demonstrated the pivotal role of AML-sEVs in promoting leukemogenesis, by facilitating the proliferation and inhibiting the apoptosis of AML cells, which are consistent with previous study.[28] Our data demonstrated that the isolated sEVs were of relative purity, but we cannot entirely exclude the possibility that some other factors were co-purified with sEVs. The noteworthy observation that sEVs treatment abolished the effect of GW4869 strongly suggests that sEVs were a major contributor. Since miRNA is an important cargo of sEVs, we performed small RNA sequencing, which revealed that miR-221 was enriched in AML-sEVs. Notably, sEVs with a high miR-221 content had a similar effect on AML cells as AML-sEVs. We also demonstrated that miR-221 accelerated leukemia progression, indicating that AML-sEVs exerted autocrine effects on AML cells, mainly via the transfer of miR-221. miR-221 has been linked to various human cancers, whereby it typically functions as an oncomiR by promoting tumor

growth,[29] lymphangiogenesis, lymphatic metastasis,[30] and angiogenesis[31,32] following its sEVs-mediated transfer. In the context of AML progression, miR-221 has emerged as a diagnostic and prognostic biomarker, while also conferring drug resistance.[33] Consistent with previous reports that miR-221 drives the expansion of leukemic cells,[34,35] the present study further demonstrated the significance of miR-221 in accelerating AML cell growth *in vitro* and leukemogenesis *in vivo*.

Although numerous investigations have focused on the paracrine effects of sEVs, their autocrine effects are less explored. Some studies have implied that tumor-derived sEVs help promote tumor metastasis and chemoresistance by acting on the same cell population.[28,36] To the best of our knowledge, sEVs prevent the RNase-mediated degradation of RNAs within it,[37] further highlighting their potential to exert autocrine effects. Although the precise mechanism through which sEVs exert their autocrine effects is not well understood, it is an important pathway that should not be overlooked when exploring the function of sEVs. Previous evidence has shown that proteins and lipids transmitted by sEVs can drive the progression of leukemia.[28,38,39] Our research provides new insights into the key miRNAs found in AML-sEVs and underscores the role of sEVs-encapsulated miRNAs in leukemia.

Our mechanistic explorations showed that miR-221 regulates *Gbp2* expression and that the proapoptotic effect of miR-221 knockdown could be rescued through *Gbp2* knockdown. Additionally, luciferase reporter analysis confirmed that *Gbp2* is targeted by miR-221, thereby substantiating the role of miR-221 in

promoting leukemogenesis through *Gbp2* modulation. As a member of the guanylate-binding protein (Gbp) family, *Gbp2* plays a role in host defense against viral and bacterial pathogens.[40-42] Although *Gbp2* is downregulated during normal erythropoiesis, it has been shown to regulate the proliferation and erythroid differentiation of TF-1 cells.[43] Moreover, *Gbp2* regulates MCL-1 and BAK to induce caspase-dependent apoptosis by inhibiting the activation of PI3K/AKT pathway.[25]

sEVs participate in paracrine communication by delivering cargos from one cell population to another, thus regulating the functions of these cells. For instance, AML-sEVs can transfer miRNAs to HSPCs to suppress their clonogenicity[44,45] or protein synthesis.[46] Simultaneously, they facilitate the formation of a tumor-permissive BM niche by modulating the proliferation, differentiation,[47-49] and angiogenesis of MSCs.[50,51] Our study also delved into the paracrine effect of AML-sEVs and found that they inhibited the colony formation ability of HSPCs, particularly their erythroid differentiation potential. miR-221-sEVs also suppressed the proliferation of HSPCs, with the highest level of miR-221 expression being detected in MEPs among all the AML mouse BM hematopoietic cells subsets. A previous study has demonstrated that miR-221 impeded the growth of erythroid cells, suggesting that it inhibits erythroid differentiation.[34]

In conclusion, our study provided evidence of the autocrine function of AML-sEVs. Moreover, we have demonstrated that AML-sEVs can transmit miR-221 to leukemic cells to promote proliferation and leukemogenesis. This

newly identified regulatory loop involving miR-221 and AML-sEVs holds great promise as a potential therapeutic target to suppress AML progression.

References

1. Shallis RM, Wang R, Davidoff A, Ma X, Zeidan AM. Epidemiology of acute myeloid leukemia: Recent progress and enduring challenges. Blood Rev. 2019;36:70-87.

2. Jaiswal S, Fontanillas P, Flannick J, et al. Age-related clonal hematopoiesis associated with adverse outcomes. N Engl J Med. 2014;371(26):2488-2498.

3. DiNardo CD, Erba HP, Freeman SD, Wei AH. Acute myeloid leukaemia. Lancet. 2023;401(10393):2073-2086.

4. Pinho S, Frenette PS. Haematopoietic stem cell activity and interactions with the niche. Nat Rev Mol Cell Biol. 2019;20(5):303-320.

5. Yuan S, Sun G, Zhang Y, Dong F, Cheng H, Cheng T. Understanding the "SMART" features of hematopoietic stem cells and beyond. Sci China Life Sci. 2021;64(12):2030-2044.

6. Zhang B, Ho YW, Huang Q, et al. Altered microenvironmental regulation of leukemic and normal stem cells in chronic myelogenous leukemia. Cancer Cell. 2012;21(4):577-592.

7. Ennis S, Conforte A, O'Reilly E, et al. Cell-cell interactome of the hematopoietic niche and its changes in acute myeloid leukemia. iScience. 2023;26(6):106943.

8. Sun G, Gu Q, Zheng J, Cheng H, Cheng T. Emerging roles of extracellular vesicles in normal and malignant hematopoiesis. J Clin Invest. 2022;132(18):e160840.

9. Schepers K, Pietras EM, Reynaud D, et al. Myeloproliferative neoplasia remodels the endosteal bone marrow niche into a self-reinforcing leukemic niche. Cell Stem Cell. 2013;13(3):285-299.

10. Zeng Z, Shi YX, Samudio IJ, et al. Targeting the leukemia microenvironment by CXCR4 inhibition overcomes resistance to kinase inhibitors and chemotherapy in AML. Blood. 2009;113(24):6215-6224.

11. Wang Y, Gao A, Zhao H, et al. Leukemia cell infiltration causes defective erythropoiesis partially through MIP-1α/CCL3. Leukemia. 2016;30(9):1897-1908.

12. Gao A, Gong Y, Zhu C, et al. Bone marrow endothelial cell-derived interleukin-4 contributes to thrombocytopenia in acute myeloid leukemia. Haematologica. 2019;104(10):1950-1961.

13. Lai JJ, Chau ZL, Chen SY, et al. Exosome Processing and Characterization Approaches for Research and Technology Development. Adv Sci. 2022;9(15):e2103222.

14. Mashouri L, Yousefi H, Aref AR, Ahadi AM, Molaei F, Alahari SK. Exosomes: composition, biogenesis, and mechanisms in cancer metastasis and drug resistance. Mol Cancer. 2019;18(1):75.

15. Slack FJ, Chinnaiyan AM. The Role of Non-coding RNAs in Oncology. Cell. 2019;179(5):1033-1055.

16. Zhou R, Chen KK, Zhang J, et al. The decade of exosomal long RNA species: an emerging cancer antagonist. Mol Cancer. 2018;17(1):75.

17. Li C, Ni YQ, Xu H, et al. Roles and mechanisms of exosomal non-coding RNAs in human health and diseases. Signal Transduct Target Ther. 2021;6(1):383.

18. Cheng H, Hao S, Liu Y, et al. Leukemic marrow infiltration reveals a novel role for Egr3 as a potent inhibitor of normal hematopoietic stem cell proliferation. Blood. 2015;126(11):1302-1313.

19. Amin AH, Sharifi LMA, Kakhharov AJ, et al. Role of Acute Myeloid Leukemia (AML)-Derived exosomes in tumor progression and survival. Biomed Pharmacother. 2022;150:113009.

20. Théry C, Amigorena S, Raposo G, Clayton A. Isolation and characterization of exosomes from cell culture supernatants and biological fluids. Current protocols in cell biology. 2006;Chapter 3:Unit 3.22.

21. Xu Y, Mou J, Wang Y, et al. Regulatory T cells promote the stemness of leukemia stem cells through IL10 cytokine-related signaling pathway. Leukemia. 2022;36(2):403-415.

22. Majoros WH, Ohler U. Spatial preferences of microRNA targets in 3' untranslated regions. BMC Genom. 2007;8:152.

23. Gu S, Jin L, Zhang F, Sarnow P, Kay MA. Biological basis for restriction of microRNA targets to the 3' untranslated region in mammalian mRNAs. Nat Struc Mol Biol. 2009;16(2):144-150.

24. Bartel DP. MicroRNAs: target recognition and regulatory functions. Cell. 2009;136(2):215-233.

25. Luo Y, Jin H, Kim JH, Bae J. Guanylate-binding proteins induce apoptosis of leukemia cells by regulating MCL-1 and BAK. Oncogenesis. 2021;10(7):54.

26. Butler JT, Abdelhamed S, Kurre P. Extracellular vesicles in the hematopoietic microenvironment. Haematologica. 2018;103(3):382-394.

27. Zhang L, Yu D. Exosomes in cancer development, metastasis, and immunity. Biochim Biophys Acta Rev Cancer. 2019;1871(2):455-468.

28. Gu H, Chen C, Hao X, et al. Sorting protein VPS33B regulates exosomal autocrine signaling to mediate hematopoiesis and leukemogenesis. J Clin Invest. 2016;126(12):4537-4553.

29. Liu W, Long Q, Zhang W, et al. miRNA-221-3p derived from M2-polarized tumor-associated macrophage exosomes aggravates the growth and metastasis of osteosarcoma through SOCS3/JAK2/STAT3 axis. Aging. 2021;13(15):19760-19775.

30. Zhou CF, Ma J, Huang L, et al. Cervical squamous cell carcinoma-secreted exosomal miR-221-3p promotes lymphangiogenesis and lymphatic metastasis by targeting VASH1. Oncogene. 2019;38(8):1256-1268.

31. Wu XG, Zhou CF, Zhang YM, et al. Cancer-derived exosomal miR-221-3p promotes angiogenesis by targeting THBS2 in cervical squamous cell carcinoma. Angiogenesis. 2019;22(3):397-410.

32. Dokhanchi M, Pakravan K, Zareian S, et al. Colorectal cancer cell-derived extracellular vesicles transfer miR-221-3p to promote endothelial cell angiogenesis via targeting suppressor of cytokine signaling 3. Life Sci.

2021;285(119937).

33. Kovynev IB, Titov SE, Ruzankin PS, et al. Profiling 25 Bone Marrow microRNAs in Acute Leukemias and Secondary Nonleukemic Hematopoietic Conditions. Biomedicines. 2020;8(12):607.

34. Felli N, Fontana L, Pelosi E, et al. MicroRNAs 221 and 222 inhibit normal erythropoiesis and erythroleukemic cell growth via kit receptor down-modulation. Proc Natl Acad Sci U S A. 2005;102(50):18081-18086.

35. Frenquelli M, Muzio M, Scielzo C, et al. MicroRNA and proliferation control in chronic lymphocytic leukemia: functional relationship between miR-221/222 cluster and p27. Blood. 2010;115(19):3949-3959.

36. Asare-Werehene M, Nakka K, Reunov A, et al. The exosome-mediated autocrine and paracrine actions of plasma gelsolin in ovarian cancer chemoresistance. Oncogene. 2020;39(7):1600-1616.

37. Koga Y, Yasunaga M, Moriya Y, et al. Exosome can prevent RNase from degrading microRNA in feces. J Gastrointest Oncol. 2011;2(4):215-222.

38. Hong CS, Jeong E, Boyiadzis M, Whiteside TL. Increased small extracellular vesicle secretion after chemotherapy via upregulation of cholesterol metabolism in acute myeloid leukaemia. j Extracll Vesicles. 2020;9(1):1800979.

39. Raimondo S, Saieva L, Corrado C, et al. Chronic myeloid leukemia-derived exosomes promote tumor growth through an autocrine mechanism. Cell Commun Signal. 2015;13:8.

40. Shenoy AR, Wellington DA, Kumar P, et al. GBP5 promotes NLRP3 inflammasome assembly and immunity in mammals. Science. 2012;336(6080):481-485.

41. Pilla DM, Hagar JA, Haldar AK, et al. Guanylate binding proteins promote caspase-11-dependent pyroptosis in response to cytoplasmic LPS. Proc Natl Acad Sci U S A. 2014;111(16):6046-6051.

42. Man SM, Karki R, Malireddi RK, et al. The transcription factor IRF1 and guanylate-binding proteins target activation of the AIM2 inflammasome by Francisella infection. Nat Immunol. 2015;16(5):467-475.

43. Lin X, Rice KL, Buzzai M, et al. miR-433 is aberrantly expressed in myeloproliferative neoplasms and suppresses hematopoietic cell growth and differentiation. Leukemia. 2013;27(2):344-352.

44. Hornick NI, Doron B, Abdelhamed S, et al. AML suppresses hematopoiesis by releasing exosomes that contain microRNAs targeting c-MYB. Sci Signal. 2016;9(444):ra88.

45. Zhao C, Du F, Zhao Y, Wang S, Qi L. Acute myeloid leukemia cells secrete microRNA-4532-containing exosomes to mediate normal hematopoiesis in hematopoietic stem cells by activating the LDOC1-dependent STAT3 signaling pathway. Stem Cell Res Ther. 2019;10(1):384.

46. Abdelhamed S, Butler JT, Doron B, et al. Extracellular vesicles impose quiescence on residual hematopoietic stem cells in the leukemic niche. EMBO Rep. 2019;20(7):e47546.

47. Kumar B, Garcia M, Weng L, et al. Acute myeloid leukemia transforms the bone marrow niche into a leukemia-permissive microenvironment through exosome secretion. Leukemia. 2018;32(3):575-587.

48. Doron B, Abdelhamed S, Butler JT, Hashmi SK, Horton TM, Kurre P. Transmissible ER stress reconfigures the AML bone marrow compartment. Leukemia. 2019;33(4):918-930.

49. Saito A, Ochiai K, Kondo S, et al. Endoplasmic reticulum stress response mediated by the PERK-eIF2(alpha)-ATF4 pathway is involved in osteoblast differentiation induced by BMP2. J Biol Chem. 2011;286(6):4809-4818.

50. Wang J, De Veirman K, Faict S, et al. Multiple myeloma exosomes establish a favourable bone marrow microenvironment with enhanced angiogenesis and immunosuppression. J Pathol. 2016;239(2):162-173.

51. Li B, Hong J, Hong M, et al. piRNA-823 delivered by multiple myeloma-derived extracellular vesicles promoted tumorigenesis through re-educating endothelial cells in the tumor environment. Oncogene. 2019;38(26):5227-5238.

Figure legends

Figure 1. Acute myeloid leukemia cells-derived small extracellular vesicles (AML-sEVs) promote AML cell growth. (A) Schematic outline of the functional experiments of AML-sEVs. Briefly, the sEVs were collected from the culture supernatant of murine primary AML cells isolated from MLL-AF9 mouse bone marrow. The impact of AML-sEVs on AML cell function was then evaluated in a co-culture system. (B-C) Evaluation of AML cell number and viability after a 3-day culture in the indicated treatment conditions. (D) Survival analysis of recipient mice injected with AML cells treated with GW4869 in the presence or absence of AML-sEVs. (E-F) Analysis of AML cell cycle and apoptosis under various treatment conditions. Data are presented as the mean ± S.D., $**p < 0.01$, $***p < 0.001$.

Figure 2. AML-sEVs promote AML cell growth by transferring miR-221 to AML cells. (A) Schematic outline of the AML-sEVs miRNA profiling experiments. sEVs collected from the bone marrow of wild type (WT) or AML mice and AML-sEVs were subjected to small RNA sequencing. Venn diagram showing the overlapping miRNAs upregulated in AML from the two small RNA sequencing experiments. (B) Heatmap of differentially expressed miRNAs between the WT and AML BM-derived sEVs (Left panel). Heatmap of differentially expressed miRNAs between WT BM-derived sEVs and AML-sEVs (Right panel). (C) Quantitative real-time PCR (qRT-PCR) analysis of differentially expressed miRNAs in sEVs. (D-E) qRT-PCR analysis of miR-221 in plasma sEVs from mice and human samples. (F) Assessment of 2×10^3 AML cell number after a 3-day incubation with miR-221-sEVs. Data are presented as

the mean ± S.D., $^{**}p < 0.01$, $^{***}p < 0.001$.

Figure 3. miR-221 knockdown inhibits leukemia development. (A) AML cell number was calculated after miR-221 knockdown (KD). (B) Representative images showing the impact on colony formation after miR-221 KD in AML cells (Left panel). Impact of miR-221 KD on AML cell colony number (Right panel). (C) Analysis of the percentage of $CD45.1^+$ AML cells in the peripheral blood (PB) of recipient mice injected with WT or miR-221 KD AML cells (n = 7-10). (D) Survival analysis of recipients injected with WT or miR-221 KD AML cells (n = 7-10). (E) Representative flow cytometry contour plots (Left panel) and corresponding bar graph showing the impact of miR-221 KD on AML cell cycle (Right panel). (F) Representative flow cytometry contour plots (Left panel) and corresponding bar graph showing the impact of miR-221 KD on AML cell apoptosis over 6 days (Right panel). $^{**}p < 0.01$, $^{***}p < 0.001$.

Figure 4. miR-221 overexpression accelerates leukemia development. (A) AML cell number was calculated after miR-221 overexpression (OE). (B) Survival analysis of recipient mice injected with WT or miR-221 OE AML cells (n = 5-8). (C-D) Graphs showing the impact of miR-221 OE on AML cell cycle and apoptosis. (E) Representative photographs of spleens from the control and miR-221 OE groups (Left panel) and comparison of spleen to body weight ratios (expressed as %) in the control and miR-221 OE groups (Right panel). (F) Representative H&E staining images of spleens from the control and miR-221 OE groups. Scale bars = 250 μm. Data are presented as the mean ± S.D., $^{*}p < 0.05$, $^{**}p < 0.01$.

Figure 5. The impact of miR-221 on other types of leukemia cells. (A) Graphs showing the impact of miR-221 KD on AML cell apoptosis (Left panel) and survival analysis of recipients injected with WT or miR-221 KD AML-ETO9a cells (n = 6-7) (Right panel). (B) Graphs illustrating the impact of miR-221 OE on AML cell apoptosis (Left panel) and survival analysis of recipients injected with WT or miR-221 OE AML-ETO9a cells (n = 6-7) (Right panel). (C-F) Analysis of the number, viability, apoptosis, and cell cycle of HL-60 cells after miR-221 KD. Data are presented as the mean ± S.D., *$p < 0.05$, ***$p < 0.001$.

Figure 6. miR-221 promotes growth of AML cell by targeting *Gbp2*. (A) Volcano plot showing significant differentially expressed genes between control and miR-221 KD AML cells (Left panel). Volcano plot showing significant differentially expressed genes between control and miR-221 OE AML cells (Right panel). (B) Venn diagram showing the overlapping genes of upregulated genes in miR-221 KD AML cells and downregulated genes in miR-221 OE AML cells. (C) A schematic diagram showing the miR-221 binding site on the 3' untranslated regions (3'UTR) of mouse *Gbp2,* which is not present in the mutated *Gbp2* 3'UTR (Left panel). The luciferase activity of cells co-transfected with miRNA NC or miR-221 mimic and the wild type (WT) or mutated (mut) *Gbp2* 3'UTR was detected (Right panel). (D) Western blotting analysis was conducted to examine the protein expression level of *Gbp2* after miR-221 KD in AML cells. (E-F) Impact of *Gbp2* KD on the proliferation and apoptosis of miR-221 KD in AML cells. Data are presented as the mean ± S.D., **$p < 0.01$, ***$p < 0.001$.

Figure 7. AML-sEVs impair erythroid differentiation of hematopoietic stem/progenitor cells (HSPCs). (A) Schematic outline of the experimental procedure used to investigate the paracrine effect of AML-sEVs on HSPCs. (B) The clonogenicity of HSPCs isolated from WT mice exposed to AML-sEVs or not was assessed by culturing in methylcellulose (Left panel). Representative images showing the colony formation of untreated and AML-sEV-treated HSPCs (Right panel). (C) Bone marrow cells from C57 mice were harvested from WT mice after the intratibial injection of AML-sEVs for 24 h. The cells were cultured in erythroid specific methylcellulose-based medium M3436 (STEM CELL) for 10-14 days. (D) Assessment of HSPCs number after a 7-day incubation with miR-221-sEVs or control-sEVs (Ctrl-sEVs). (E) qRT-PCR analysis of miR-221 expression in mouse hematopoietic cell populations: long-term hematopoietic stem cells (LT-HSCs), short-term hematopoietic stem cell (ST-HSCs), multipotent progenitors (MPPs), common myeloid progenitors (CMPs), common lymphoid progenitors (CLPs), granulocyte-macrophage progenitors (GMPs), megakaryocyte-erythroid progenitors (MEPs), and megakaryocyte progenitors (MkPs) from the WT and AML mouse bone marrow. (F) $Lin^{-}cKit^{+}$ cells were harvested from WT mice after the intratibial injection of PBS, ctrl-sEVs or miR-221KD-sEVs for 24 h. The cells were cultured in methylcellulose-based medium M3434 (STEM CELL) for 7-10 days. Data are presented as the mean ± S.D., $*p < 0.05$, $**p < 0.01$, $***p < 0.001$.

Figure 1

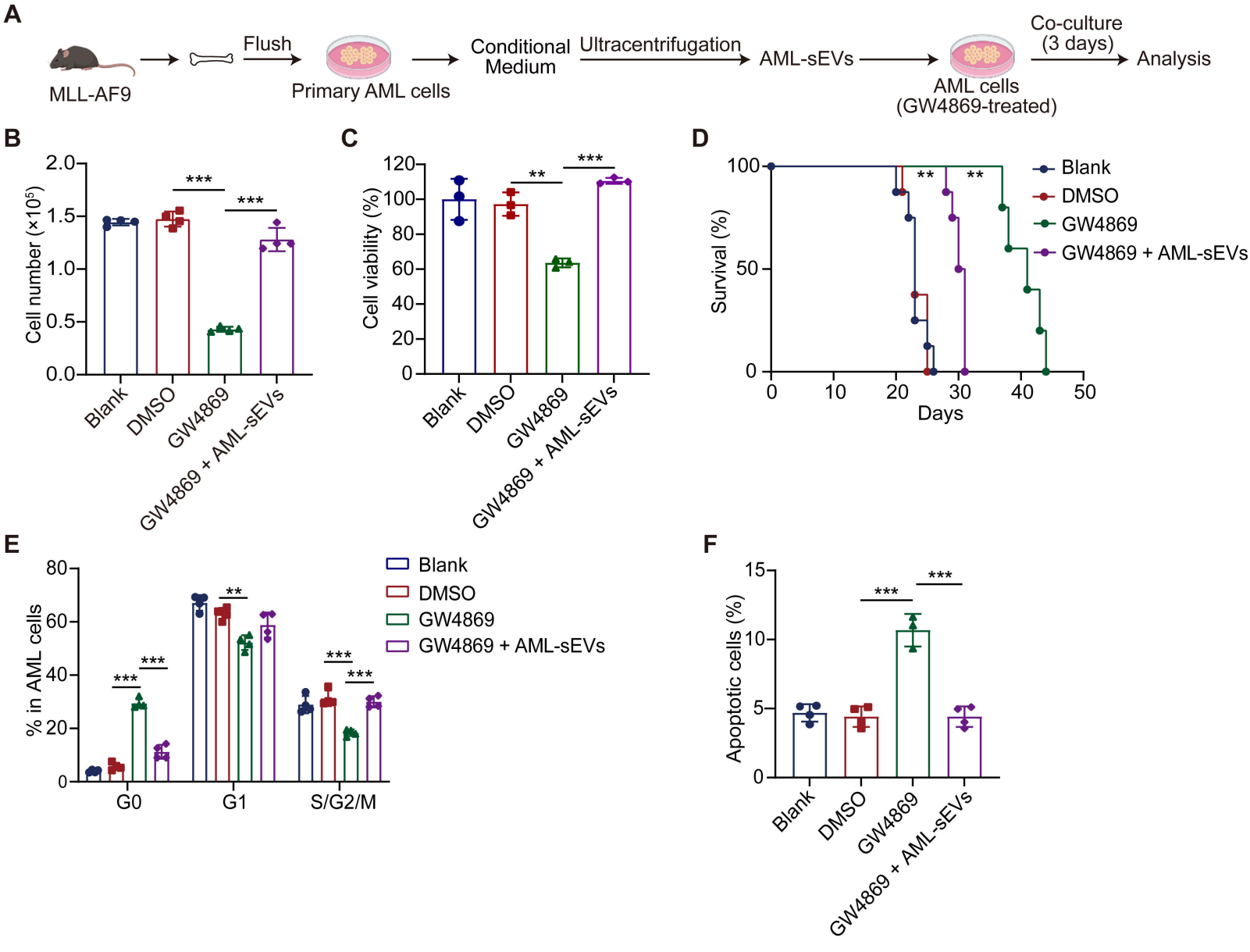
A
MLL-AF9
Flush
Primary AML cells
Conditional Medium
Ultracentrifugation
AML-sEVs
AML cells (GW4869-treated)
Co-culture (3 days)
Analysis
B
Cell number (×10^5)
2.0
1.5
1.0
0.5
0.0
***
***
Blank
DMSO
GW4869
GW4869 + AML-sEVs
C
Cell viability (%)
120
100
80
60
40
20
0
**
***
Blank
DMSO
GW4869
GW4869 + AML-sEVs
D
Survival (%)
100
50
0
**
**
0
10
20
30
40
50
Days
Blank
DMSO
GW4869
GW4869 + AML-sEVs
E
% in AML cells
80
60
40
20
0
***
***
**
***
***
G0
G1
S/G2/M
Blank
DMSO
GW4869
GW4869 + AML-sEVs
F
Apoptotic cells (%)
15
10
5
0
***
***
Blank
DMSO
GW4869
GW4869 + AML-sEVs

Figure 2

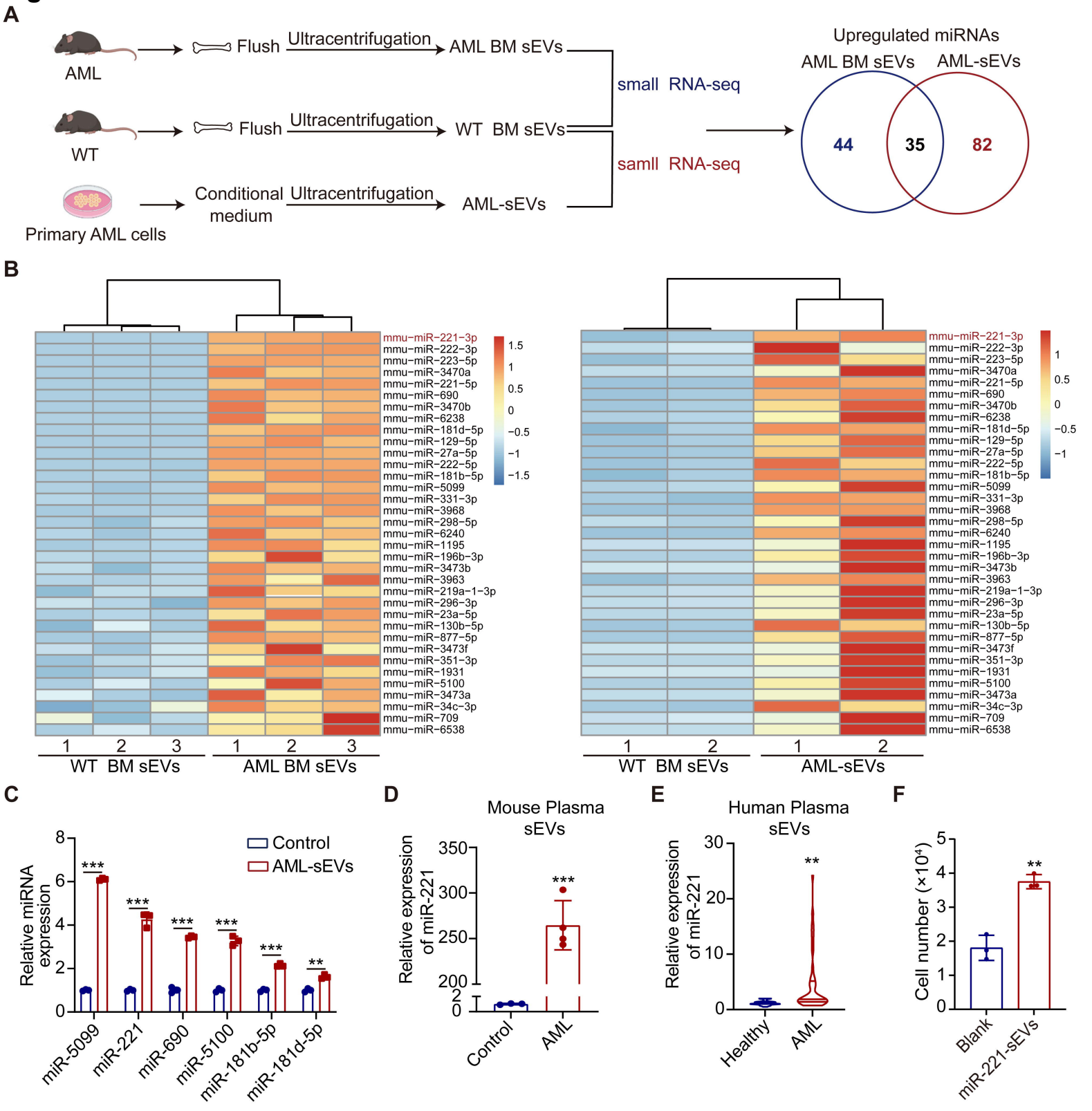
A
AML
Flush
Ultracentrifugation
AML BM sEVs
WT
Flush
Ultracentrifugation
WT BM sEVs
Primary AML cells
Conditional medium
Ultracentrifugation
AML-sEVs
small RNA-seq
samll RNA-seq
Upregulated miRNAs
AML BM sEVs
AML-sEVs
44
35
82
B
mmu-miR-221-3p
mmu-miR-222-3p
mmu-miR-223-5p
mmu-miR-3470a
mmu-miR-221-5p
mmu-miR-690
mmu-miR-3470b
mmu-miR-6238
mmu-miR-181d-5p
mmu-miR-129-5p
mmu-miR-27a-5p
mmu-miR-222-5p
mmu-miR-181b-5p
mmu-miR-5099
mmu-miR-331-3p
mmu-miR-3968
mmu-miR-298-5p
mmu-miR-6240
mmu-miR-1195
mmu-miR-196b-3p
mmu-miR-3473b
mmu-miR-3963
mmu-miR-219a-1-3p
mmu-miR-296-3p
mmu-miR-23a-5p
mmu-miR-130b-5p
mmu-miR-877-5p
mmu-miR-3473f
mmu-miR-351-3p
mmu-miR-1931
mmu-miR-5100
mmu-miR-3473a
mmu-miR-34c-3p
mmu-miR-709
mmu-miR-6538
1.5
1
0.5
0
−0.5
−1
−1.5
1 2 3 1 2 3
WT BM sEVs
AML BM sEVs
1 2 1 2
WT BM sEVs
AML-sEVs
C
Control
AML-sEVs
Relative miRNA expression
***
***
***
***
***
**
miR-5099
miR-221
miR-690
miR-5100
miR-181b-5p
miR-181d-5p
D
Mouse Plasma sEVs
Relative expression of miR-221
***
Control
AML
E
Human Plasma sEVs
Relative expression of miR-221
**
Healthy
AML
F
Cell number (×10⁴)
**
Blank
miR-221-sEVs

Figure 3

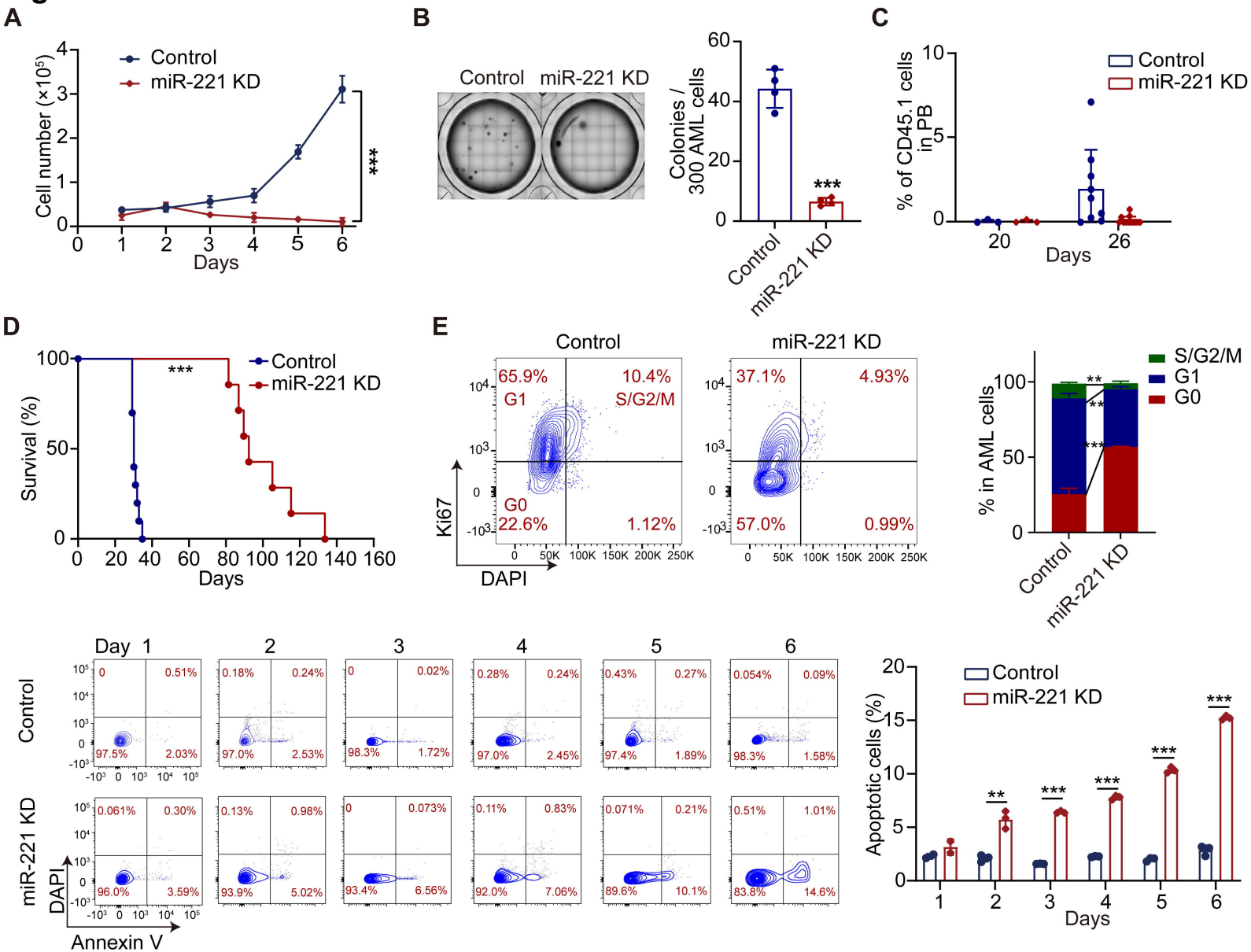
A
Control
miR-221 KD
Cell number (×10⁵)
Days
***
B
Control
miR-221 KD
Colonies / 300 AML cells
***
C
Control
miR-221 KD
% of CD45.1 cells in PB
Days
D
Control
miR-221 KD
Survival (%)
***
Days
E
Control
miR-221 KD
65.9%
G1
10.4%
S/G2/M
22.6%
G0
1.12%
37.1%
4.93%
57.0%
0.99%
Ki67
DAPI
S/G2/M
G1
G0
% in AML cells
Day 1
2
3
4
5
6
Control
miR-221 KD
DAPI
Annexin V
Apoptotic cells (%)
Days

Figure 4

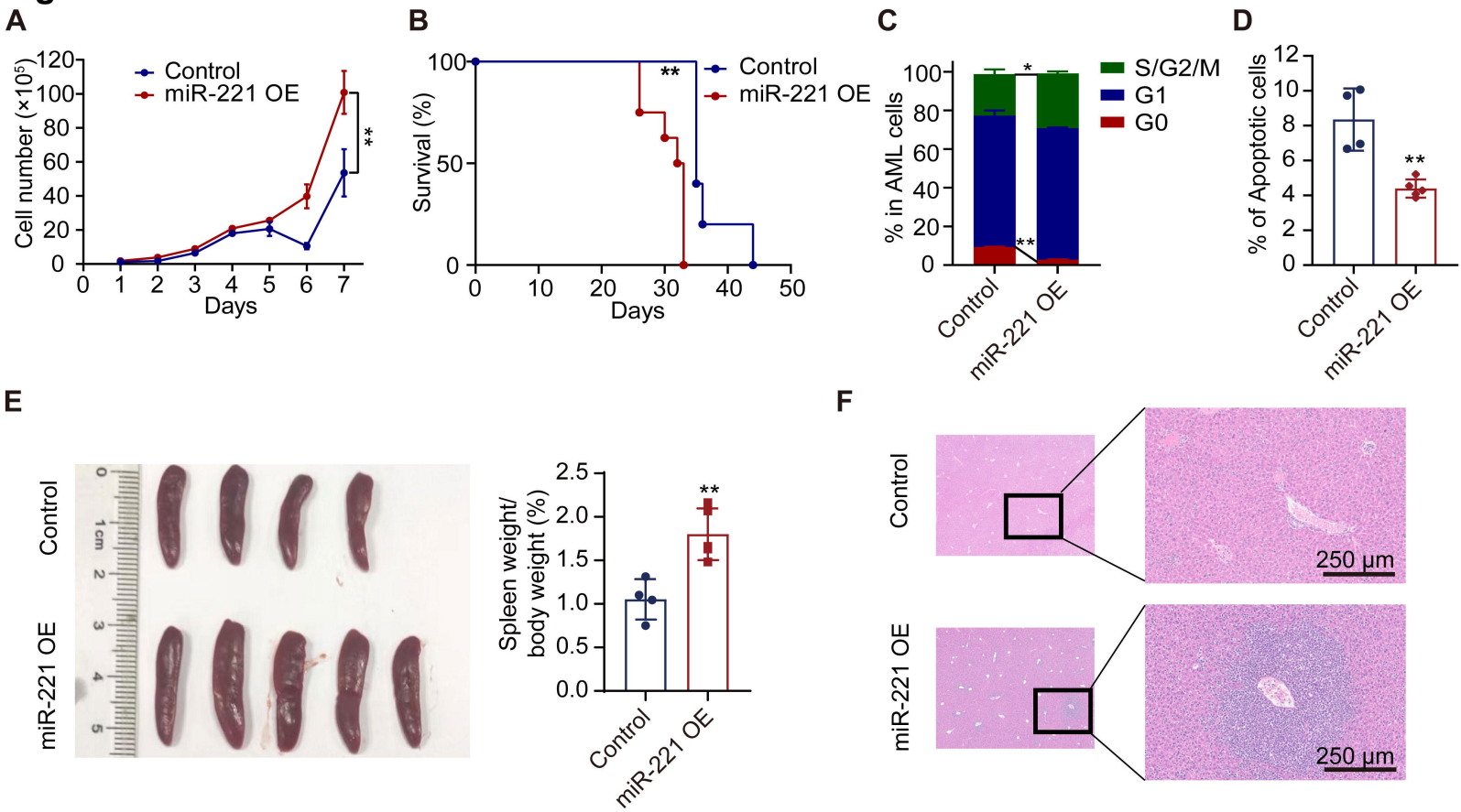
A
Control
miR-221 OE
Cell number (×10^5)
Days
**
B
Control
miR-221 OE
Survival (%)
Days
**
C
S/G2/M
G1
G0
% in AML cells
*
**
Control
miR-221 OE
D
% of Apoptotic cells
**
Control
miR-221 OE
E
Control
miR-221 OE
Spleen weight/ body weight (%)
**
Control
miR-221 OE
F
Control
miR-221 OE
250 μm
250 μm

Figure 5

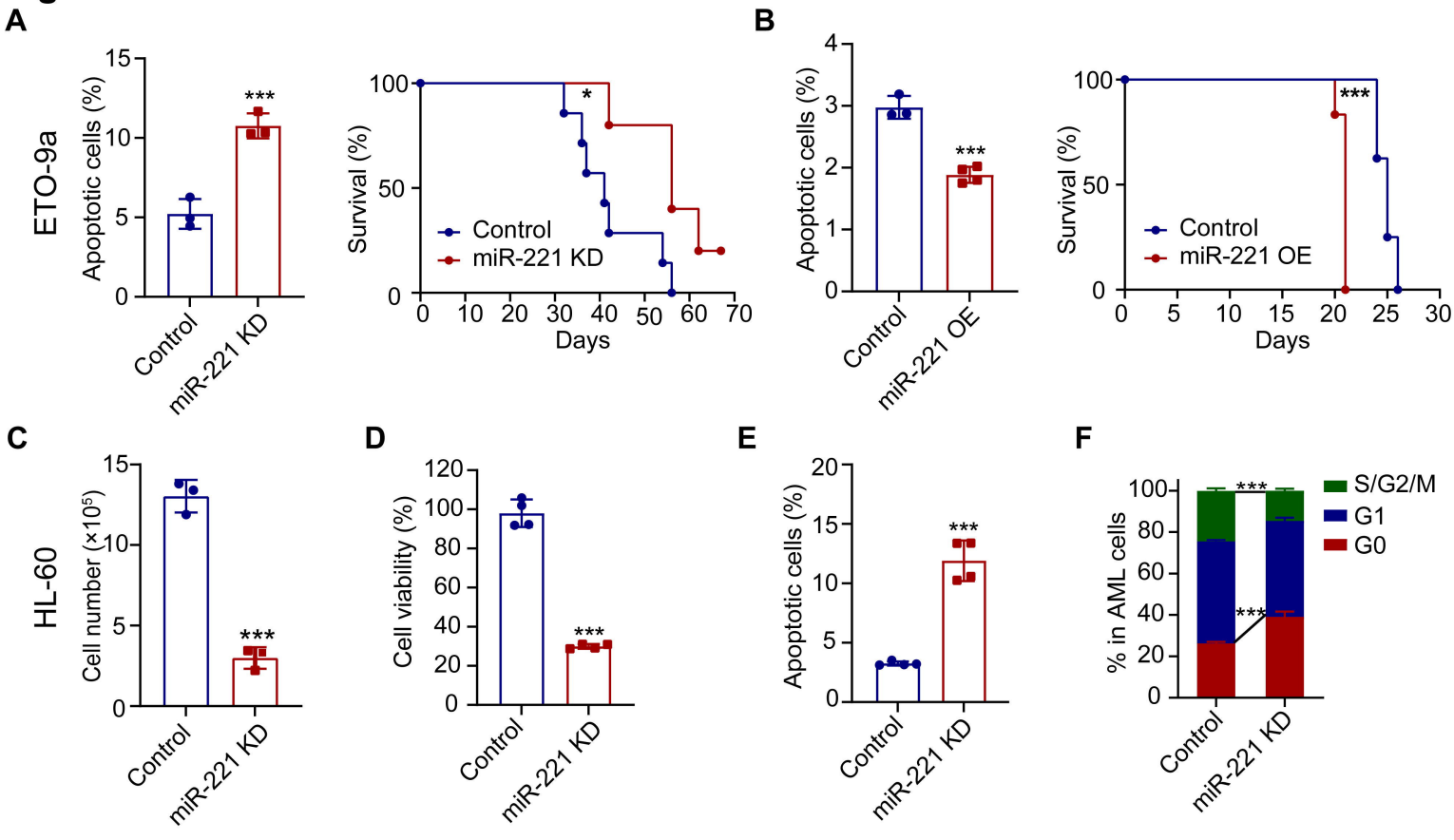
A
ETO-9a
Apoptotic cells (%)
15
10
5
0
***
Control
miR-221 KD
Survival (%)
100
50
0
*
Control
miR-221 KD
0 10 20 30 40 50 60 70
Days
B
Apoptotic cells (%)
4
3
2
1
0
***
Control
miR-221 OE
Survival (%)
100
50
0
***
Control
miR-221 OE
0 5 10 15 20 25 30
Days
C
HL-60
Cell number (×10⁵)
15
10
5
0
***
Control
miR-221 KD
D
Cell viability (%)
120
100
80
60
40
20
0
***
Control
miR-221 KD
E
Apoptotic cells (%)
20
15
10
5
0
***
Control
miR-221 KD
F
% in AML cells
100
80
60
40
20
0
***
***
S/G2/M
G1
G0
Control
miR-221 KD

Figure 6

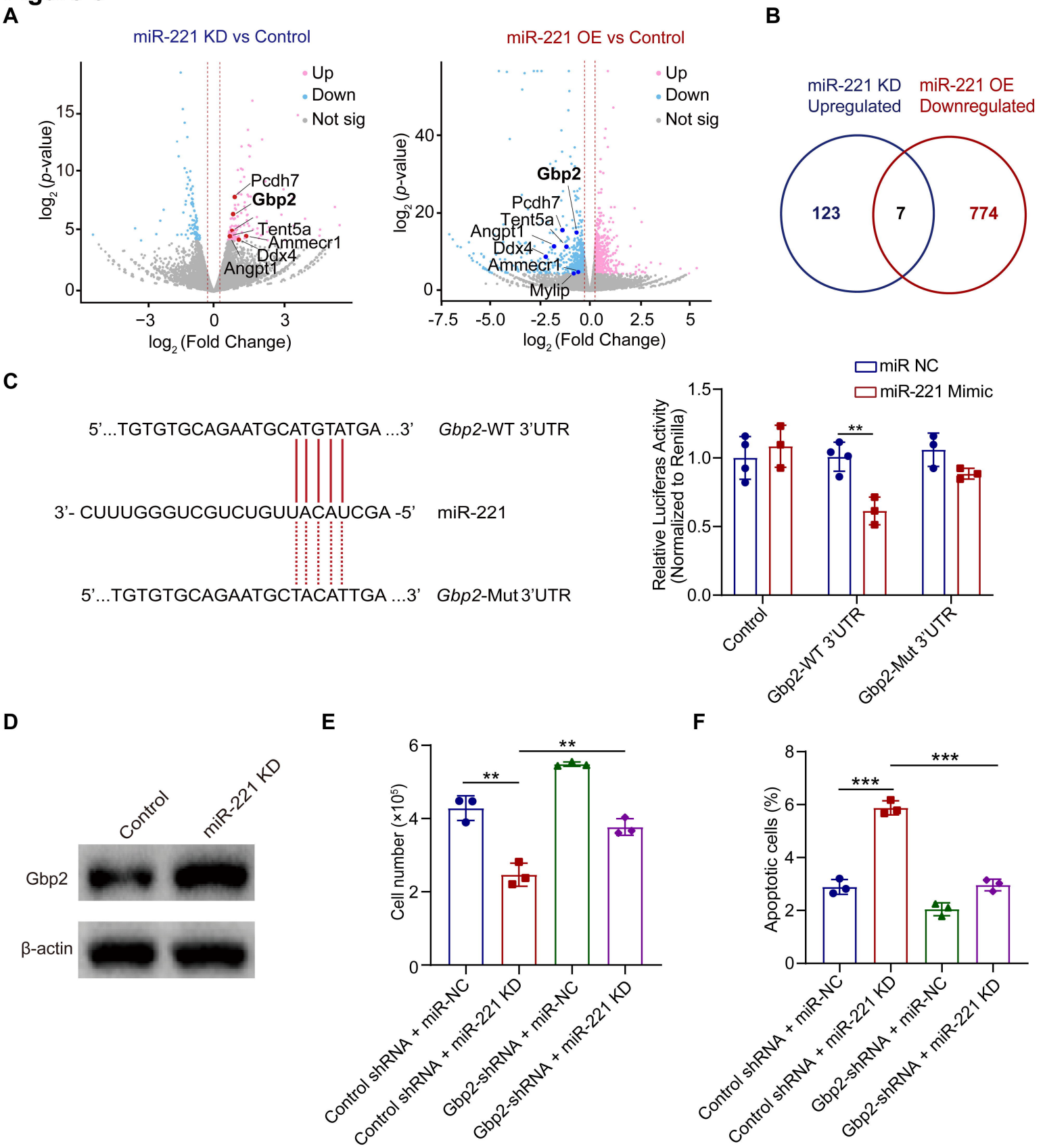
A
miR-221 KD vs Control
Up
Down
Not sig
log2 (p-value)
log2 (Fold Change)
Pcdh7
Gbp2
Tent5a
Ammecr1
Ddx4
Angpt1
miR-221 OE vs Control
Up
Down
Not sig
log2 (p-value)
log2 (Fold Change)
Gbp2
Pcdh7
Tent5a
Angpt1
Ddx4
Ammecr1
Mylip
B
miR-221 KD Upregulated
miR-221 OE Downregulated
123
7
774
C
5'...TGTGTGCAGAATGCATGTATGA ...3' Gbp2-WT 3'UTR
3'- CUUUGGGUCGUCUGUUACAUCGA -5' miR-221
5'...TGTGTGCAGAATGCTACATTGA ...3' Gbp2-Mut 3'UTR
miR NC
miR-221 Mimic
Relative Luciferas Activity (Normalized to Renilla)
**
Control
Gbp2-WT 3'UTR
Gbp2-Mut 3'UTR
D
Control
miR-221 KD
Gbp2
β-actin
E
Cell number (×10⁵)
**
**
Control shRNA + miR-NC
Control shRNA + miR-221 KD
Gbp2-shRNA + miR-NC
Gbp2-shRNA + miR-221 KD
F
Apoptotic cells (%)
***
***
Control shRNA + miR-NC
Control shRNA + miR-221 KD
Gbp2-shRNA + miR-NC
Gbp2-shRNA + miR-221 KD

Figure 7

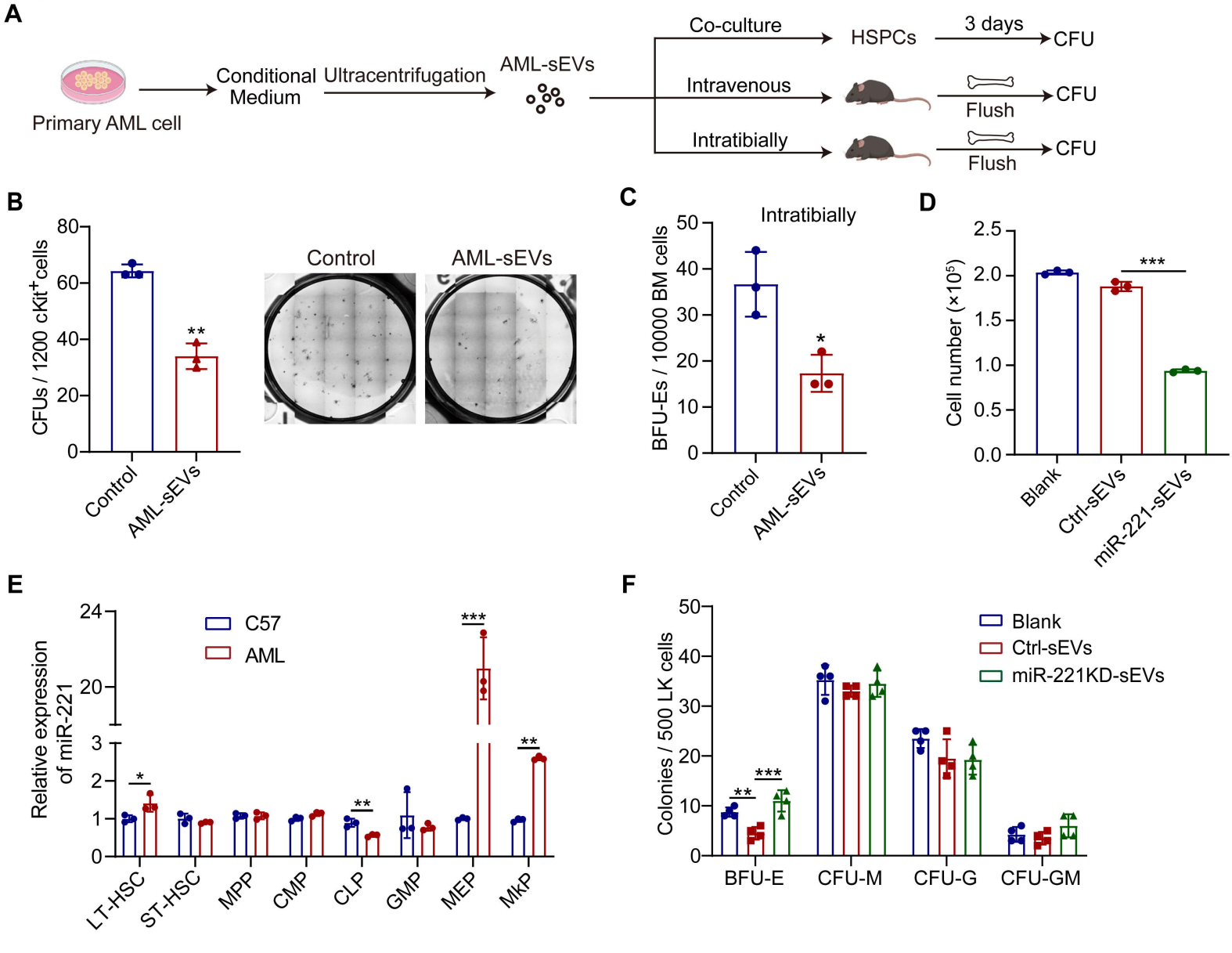
A
Primary AML cell
Conditional Medium
Ultracentrifugation
AML-sEVs
Co-culture
HSPCs
3 days
CFU
Intravenous
Flush
CFU
Intratibially
Flush
CFU
B
CFUs / 1200 cKit+ cells
Control
AML-sEVs
C
Intratibially
BFU-Es / 10000 BM cells
Control
AML-sEVs
D
Cell number (×10⁵)
Blank
Ctrl-sEVs
miR-221-sEVs
E
Relative expression of miR-221
C57
AML
LT-HSC
ST-HSC
MPP
CMP
CLP
GMP
MEP
MkP
F
Colonies / 500 LK cells
Blank
Ctrl-sEVs
miR-221KD-sEVs
BFU-E
CFU-M
CFU-G
CFU-GM

Small extracellular vesicles derived from acute myeloid leukemia cells promote leukemogenesis by transferring miR-221-3p

Supplementary Information:

Supplementary Methods

Supplementary Method References

Supplementary Figure Legends

Supplementary Table 1

Supplementary Table 2

Supplementary Methods:

Cell culture

Primary murine AML cells were isolated from the bone marrow of MLL-AF9 AML mice as previously described.[1] AML cells were cultured in IMDM medium containing 10 ng/mL mouse interleukin (IL)-3 (Peprotech), 10 ng/mL mouse IL-6 (Peprotech), 50 ng/mL mouse stem cell factor (SCF) (Peprotech), 15% fetal bovine serum (FBS), and 1% penicillin and streptomycin (Gibco). HEK293T cells were cultured in high-glucose DMEM medium containing 10% FBS and 1% penicillin and streptomycin. THP-1, HL-60, Kasumi-1 and MOLM-13 cells were cultured in RPMI-1640 medium containing 10% FBS and 1% penicillin and streptomycin. All cells were maintained in an incubator with 5% CO_2 at 37 °C.

sEVs isolation, characterization, and quantification

To obtain sEVs-free fetal bovine serum (FBS), equal volumes of medium (IMDM or DMEM) and FBS were combined and the mixture was ultracentrifuged at 110 000 ×g at 4 °C overnight. To obtain the conditioned medium (CM), cells were washed with phosphate-buffered saline (PBS) three times and resuspended with sEVs-free medium. After 48 h, the CM was collected and sequentially centrifuged at 300 ×g for 10 min, 2 000 ×g for 10 min, and finally at 10 000 ×g for 30 min to remove the dead cells, cellular debris, and large vesicles, respectively. The supernatant was then filtered using a 0.22-μm filter followed by ultracentrifugation at 110 000 ×g for 70 min to obtain sEVs pellets. The

pellets were washed with PBS once and subjected to a final ultracentrifugation step at 110 000 ×g for 70 min to ensure the purification of sEVs. All centrifugation steps were conducted at 4 °C. After the sEVs were resuspended in PBS, protein concentration was detected using a BCA assay. The morphology and size of sEVs were evaluated using a transmission electron microscope (HT7700 Exalens, Tokyo, Japan). The quantity and size distribution of sEVs were assessed using the Zetasizer NanoSampler ZS90 (Malvern Panalytical, Malvern, UK). The sEVs-specific proteins CD9, CD63, and TSG101, and the endoplasmic-reticulum-derived protein Calnexin were detected by western blotting.

Human peripheral blood (PB) collection and plasma processing

This study was approved by the Ethics Committee according to the regulations of the institutional ethics review boards from the Institute of Hematology and Blood Diseases Hospital, Chinese Academy of Medical Sciences and Peking Union Medical College, informed consent was signed by all patients. Human PB samples from 25 healthy control and 41 AML patients were obtained from The First People's Hospital of Yunnan Province. PB were collected in EDTA blood tubes and centrifuged at 2 000 ×g for 10 min to separate the plasma fraction. Subsequently, add an equal volume of pre-cooled PBS to the plasma and the mixture was further ultracentrifuged to isolate sEVs.

AML cell proliferation assay

To examine the impact of sEVs on AML cells, AML cells were cultured in sEVs-free culture medium, supplemented with 10 μg/mL of sEVs, and co-cultured for 3 days prior to transplantation into mice or proliferation analysis. To investigate the effect of GW4869 (MCE) on sEVs and AML cells, it was used at a concentration of 5 μM to inhibit sEV release. Before co-culturing with sEVs, AML cells were pre-treated with GW4869 for 24 h. To investigate the effect of miR-221 or *Gbp2* on AML cells, AML cells were infected with lentivirus for 48 h, cell cycle was analyzed. Cell proliferation and cell apoptosis were measured for 6 consecutive days. Cell viability was assessed by the CCK-8 assay (DOJINDO) following the manufacturer's instructions.

HSPCs co-culture and PKH67 labeling

For the in vitro sEVs treatment, BM cells from WT mouse were enriched using CD117 Microbeads (Miltenyi) and 1×10^3 $cKit^+$ cells were cultured in a 48-well plate with 800 μL of StemSpan serum-free medium (STEMCELL Technologies), supplemented with 100 ng/mL mouse SCF (Peprotech), 100 ng/mL mouse TPO (Peprotech) along with 8 μg of AML-sEVs for 7 days. To visualize the internalization of sEVs by HSPCs, AML-sEVs were labeled with PKH67 according to manufacturer’s instructions. Briefly, sEVs pellet was resuspend with 1 mL of Diluent C, then 4 μL of the PKH67 dye solution was added and mixed thoroughly. After incubating the mixture for 5 minutes, 2 mL of 1% bovine

serum albumin serum was added to allow binding of excess dye. The sEVs were then centrifuged at 110 000 ×g for 70 minutes at 4°C, and sEVs pellet was resuspended for collection. The labeled sEVs were cultured with 1×10^5 $ckit^+$ cells. After 12 h, the sEV-treated HSPCs were cytospined and imaged using a laser-scanning confocal microscope.

In vitro erythroid differentiation assay

To assess the erythroid differentiation ability of HSPCs, 50 $cKit^+$ cells were sorted and cultured in a 96-well plate with 200 μL of Minimum Essential Medium (α-MEM, Gbico). The medium was supplemented with 10 ng/mL mouse SCF, 10 ng/mL mouse TPO (Peprotech) ,10 ng/mL mouse IL-3 (Peprotech), 1 IU/mL human EPO (Peprotech), 2 mM L-Glutamine, 50 U/mL penicillin-streptomycin solution and 15% sEVs-free fetal bovine serum, along with different concentration of AML-sEVs (10, 50 μg/mL) for 3 weeks. Erythroid differentiation ability was detected by Flow cytometry.

Colony formation assay

After 48 h of AML cells infection, GFP^+ or $mCherry^+$ cells were sorted into MethoCult M3231 (StemCell Technologies), a methylcellulose-based medium, supplemented with 50 ng/mL mouse stem cell factor (SCF), 10 ng/mL mouse IL-6, 10 ng/mL mouse IL-3, and 1% penicillin/streptomycin (all purchased from PeproTech). Colonies were observed and quantified after 7-10 days of culture. Murine BM cells or $cKit^+$ HSPCs were cultured in MethoCult M3434 medium (StemCell Technologies) for 7-10 days to generate CFU-G, CFU-M, CFU-GM,

and CFU-GEMM colonies. To form BFU-E colonies, the BM cells were cultured in MethoCult M3436 medium (StemCell Technologies) for 10-14 days.

RNA oligonucleotides, plasmids

RNA oligonucleotides were synthesized by RiboBio (Guangzhou, China), the oligos used in this study are listed in Supplementary Table 2. The anti-miR plasmid is custom made to specifically target miR-221-3p, which was generated by ligation of double stranded oligo's sense/antisense into the BamHI and EcoRI restriction sites of the miRZIP pGreen-Puro Lentiviral-based miRNA inhibition vector. The nucleotides for the specific anti-microRNA sequence targeting the miR-221-3p are shown: 5'-GAAACCCAGCAGACAATGTAGCT-3'. Green fluorescent protein (GFP) was used as the positive sorting reporter. The miR-221-overexpressing plasmid was constructed as previously described.[2] Oligos (synthesized by Tsingke) were annealed and ligated into the AgeI- and BamHI-digested GV298 plasmid, which was purchased from GeneChem (Shanghai, China). mCherry was used as the positive sorting reporter.

Lentivirus package and transfection

The lentiviral vectors, pSPAX2, and pMD2.G packaging plasmids were mixed at a 7:5:3 mass ratio and transfected into 293T cells using the Lipofectamine 2000 Transfection Reagent (Invitrogen). After 48-72 h, the lentivirus was collected and concentrated at 20 000 ×g for 2.5 h at 4 °C. For cell infection, 5×10^5 cells

were transferred to a vitronectin-coated 24-well plate and incubated with the lentivirus and 8 μg/mL polybrene (Sigma-Aldrich). The plate was centrifuged for 90 min at 1800 rpm and 37 °C, and the medium was replenished after 8-12 h.

Limiting Dilution Assays (LDAs)

For in vivo LDAs, murine MLL-AF9 AML cells were transduced with either control or miR-221-overexpressed lentivirus. Recipients (n = 9 for each group) were irradiated with 5.0 Gy before being transplanted with four doses of leukemia cells for each group. The number of recipient mice that developed leukemia post-transplantation within 110 days were record in each group. The frequency of LSCs was analyzed by Extreme Limiting Dilution Analysis (ELDA) with online tool: http://bioinf.wehi.edu.au/software/elda/.[3]

Western blotting

Proteins from cells or sEVs were isolated using sodium dodecyl sulfate buffer, separated on a 10% polyacrylamide gel, and subsequently transferred onto PVDF membranes. After blocking the membranes with 5% bovine serum albumin for 1 h at room temperature, the membranes were incubated overnight with primary antibodies at 4 °C. The following day, the membranes were washed with PBST and then incubated with a horseradish-peroxidase-conjugated secondary antibody to detect the chemiluminescence signals. The primary antibodies used in this study are as

follows: CD63 (ab216130, Abcam), CD9 (ab92726, Abcam), TSG101 (ab125011, Proteintech), Calnexin (ab22595, Abcam), Gbp2 (11854-1-AP, Proteintech), β-actin (A1978, Sigma-Aldrich), BAX (A0207, ABclonal) and anti-AKT (9272), anti-phospho-AKT (4058), anti-SAPK/JNK (9252), anti-phospho-SAPK/JNK (9251) antibodies were purchased from Cell Signaling Technology.

RNA extraction and qRT-PCR

RNA was extracted from sEVs using the miRNeasy Kit (217004, QIAGEN) and from cells using the Trizol reagent (Invitrogen). For the miRNA analysis, the miRNA was reverse-transcribed using the miRNA First-Strand Synthesis Kit (Takara, 638313) and subjected to qRT-PCR analysis using the miRNA TB Green Kit (Takara, 638314). Meanwhile, mRNA was reverse-transcribed into cDNA using the HiScriptII 1st strand cDNA synthesis kit (Vazyme, R211) and subjected to qRT-PCR analysis using the SYBR qPCR Master Mix (Vazyme, Q711). The qRT-qPCR was conducted on a QuantStudio5 system (Applied Biosystems). *U6* or *GAPDH* were used as internal reference for detecting miRNA or mRNA, respectively, in cells and sEVs. The primers used for qRT-PCR can be found in Supplementary Table 1.

Dual-luciferase reporter assay

To generate the dual-luciferase reporter vectors, the full-length 3′UTR

sequences from the selected AML-associated genes were PCR-amplified and inserted between the SacI and XhoI restriction sites of the pmirGLO dual-luciferase miRNA target expression vector (Promega) using the Basic Seamless Cloning and Assembly Kit (TransGen Biotech). A mutated *Gbp2* 3′UTR sequence with a mutation at positions of the miRNA seed sequence, as described in the main text, was synthesized by GENEWIZ. The pmirGLO vector expressed firefly luciferase, with *Renilla* luciferase serving as the internal reference. 293T cells (1.2×10^5 cells) were seeded in 24-well plates and co-transfected with reporter plasmids containing the 3'UTR of the target gene and either a negative control miRNA (miR NC) or an miR-221 mimic using Lipofectamine 3000 and the Lipofectamine RNAiMAX Transfection Reagent (Invitrogen), respectively. Cell lysates were collected after 36 h, and luciferase activity was measured using a microplate reader according to the manufacturer's instructions (Promega).

Small RNA sequencing and analyses

Each experimental group comprised two or three technical replicates. Once collected, the sEVs were sent to RiboBio Co., Ltd. (Guangzhou, China) for high-throughput miRNA sequencing. The RNA was extracted by trizol and the libraries of small RNAs were constructed using TruSeq Small RNA Library Preparation Kits (Illumina) according to the manufacturers' instructions, followed by sequencing by Illumina HiSeq 2500 platform. Raw data (raw reads)

underwent initial filtration, involving the removal of joints at both ends of reads. Additionally, the reads with fragment length less than 17nt and low-quality reads are removed to obtain high-quality data (clean reads). Clean reads were mapped to the mouse genome (GRCm38) using Bowite 2.2.5. The differential miRNA expression analysis was carried out using DESeq2. For miRNA with significant differences, the target genes of miRNA will be further predicted, and the target genes were enriched by gene ontology (GO) and KEGG biological pathway analyses.

RNA sequencing and analyses

For transcriptome sequencing, MLL-AF9 AML cells were infected with control or miR-221 knockdown/overexpressing lentivirus. After 48 h, cells were sorted by flow cytometry and lysed in Trizol reagent to extract RNA. The cDNA libraries were prepared using an Illumina RNA library preparation kit and sequenced by the Illumina NovaSeq 6000 in Novogene Co. (Tianjin, China). Differential gene expression analyses were conducted using the DESeq2 R package with Padj < 0.05 and Foldchange > 1.2 were set as the threshold for significant differential expression.

Supplementary Method References:

1. Cheng H, Hao S, Liu Y, et al. Leukemic marrow infiltration reveals a novel role for Egr3 as a potent inhibitor of normal hematopoietic stem cell proliferation. Blood. 2015;126(11):1302-1313.

2. Wang XW, Hao J, Guo WT, et al. A DGCR8-Independent Stable MicroRNA Expression Strategy Reveals Important Functions of miR-290 and miR-183-182 Families in Mouse Embryonic Stem Cells. Stem cell reports. 2017;9(5):1618-1629.

3. Hu Y, Smyth GK. ELDA: extreme limiting dilution analysis for comparing depleted and enriched populations in stem cell and other assays. Journal of immunological methods. 2009;347(1-2):70-78.

Supplementary Figure Legends:

Figure S1. Identification of acute myeloid leukemia cells-derived small extracellular vesicles (AML-sEVs) and their role on AML cells. (A) Transmission electron microscopy image of sEVs isolated from AML cells. (B) Nanoparticle tracking analysis was used to determine the size and number of sEVs isolated from AML cells. (C) Western blotting showing the protein expression level of Calnexin, TSG101, CD63, and CD9 in AML-sEVs and AML cells. Calnexin is an endoplasmic reticulum membrane marker. TSG101, CD63, and CD9 are sEV-specific markers. (D) AML cells were quantified after incubation with or without AML-sEVs for 3 days. (E-F) Flow cytometric analysis of Ki67-APC and Annexin-V-APC staining in AML cells treated with GW4869 for 3 days, in the presence or absence of AML-sEVs. Data are presented as the mean ± S.D., ***$p < 0.001$.

Figure S2. miRNA quantification in sEVs and AML cells. (A-C) Quantitative real-time PCR (qRT-PCR) analysis of differentially expressed miRNAs in sEVs and AML cells. (D) Conservation analysis of the miR-221 sequence across various species. Data are presented as the mean ± S.D., *$p < 0.05$, **$p < 0.01$.

Figure S3. Impact of miR-221-sEVs on AML cells. (A-B) qRT-PCR analysis of miR-221 in miR-221-ovexpressing 293T cells and sEVs. (C-D) Evaluation of AML cell number and viability after exposure to the indicated treatment

conditions. (E-F) Analysis of AML cell cycle and apoptosis after a 3-day co-culture with miR-221-sEVs. (G-H) Flow cytometric analysis of Ki67-APC and Annexin-V-APC staining in AML cells treated with GW4869 for 3 days, in the presence or absence of Ctrl-sEVs or miR-221-sEVs. Data are presented as the mean ± S.D., ***$p < 0.001$.

Figure S4. Impact of miR-221 overexpression on leukemogenesis. (A) Colony numbers were determined after miR-221 overexpression (OE). (B) Analysis of the percentage of CD45.1$^+$ AML cells in the peripheral blood (PB) of recipient mice injected with wild-type (WT) or miR-221 OE AML cells (n = 5-8). (C-E) Representative photographs, liver to body weight ratios, and H&E staining images of control and miR-221 OE mouse livers. (F-G) Bar graph and flow cytometric analysis of the frequency of leukemic granulocyte macrophage progenitors (L-GMPs) in the BM of recipients injected with WT or miR-221 OE AML cells (n = 5-8). (H) The in vivo limiting dilution assay was conducted using leukemia cells transduced with either control or miR-221-overexpressed lentivirus. Left (up): Table showing the doses of leukemia cells and the corresponding number of recipients that developed leukemia. Left (down): the estimated leukemia stem cells (LSCs) frequency was analyzed. Right: Log fraction plot showing the LSCs frequency. Recipients (n = 9 for each group) were irradiated with 5.0 Gy before transplanted with different doses of leukemia cells and the estimated LSCs frequency was analyzed by ELDA. Data are

presented as the mean ± S.D., $^{**}p < 0.01$. ns, no significant differences.

Figure S5. miR-221 transfer by AML-sEVs. (A-B) qRT-PCR analysis of miR-221 in miR-221 KD AML cells and their sEVs. (C-D) qRT-PCR analysis of miR-221 in miR-221 OE AML cells and their sEVs. (E-F) Evaluation of the number or apoptosis of control and miR-221 KD AML cells cultured with or without miR-221-sEVs. (G) Representative flow cytometry contour plots of Annexin-V staining. Data are presented as the mean ± S.D., $^{*}p < 0.05$, $^{**}p < 0.01$, $^{***}p < 0.001$.

Figure S6. Impact of miR-221 knockdown on Human leukemia cells. (A) Analysis of number, viability, apoptosis, and cell cycle of THP-1 cells after miR-221 knockdown (KD). (B) Analysis of number, viability, apoptosis, and cell cycle of Kasumi-1 cells after miR-221 KD. (C) Analysis of number, viability, apoptosis, and cell cycle of MOLM-13 cells after miR-221 KD. Data are presented as the mean ± S.D., $^{**}p < 0.01$, $^{***}p < 0.001$.

Figure S7. Gbp2 promotes the proliferation of AML cells. (A) Heatmap of differentially expressed genes between the control and miR-221 KD AML cells. (B) Heatmap of differentially expressed genes between the control and miR-221 OE AML cells. (C) Geno Ontology (GO) enrichment analyses of miR-221 target genes predicted by TargetScan, miRTarBase, miRWalk, and miRDB. (D) The

luciferase activity of miR NC or miR-221 mimic co-transfected with gene-3' untranslated regions (3'UTR)-expressing vector into 293T cells. (E) qRT-PCR analysis to evaluate the expression level of *Gbp2*. (F) qRT-PCR analysis to evaluate the knockdown efficiency of *Gbp2*. (G-H) Evaluation of the proliferation and apoptosis after Gbp2 KD in AML cells. (I) Western blotting was conducted to examine the indicate protein expression level in control- or Gbp2-overexpressed AML cells. Data are presented as the mean ± S.D., *$p < 0.05$, **$p < 0.01$, ***$p < 0.001$.

Figure S8. The effect of AML-sEVs on hematopoietic stem/progenitor cells (HSPCs). (A) Confocal microscopy for GFP^+ sEVs in the cytosol of HSPCs after co-culture with PKH67-labeled sEVs for 12 h. DAPI, 4′,6-diamidino-2-phenylindole. (B) Number of HSPCs was assessed after a 7-day co-culture with AML-sEVs. (C) Evaluating the clonogenicity of $cKit^+$ HSPCs isolated from WT mice intravenously injected with AML-sEVs or PBS. (D) Analysis of the percentage of $Ter119^+$ cells. (E) qRT-PCR analysis of miR-221 expression in HSPCs, mesenchymal stem cells (MSCs) and endothelial cells (ECs). (F) Cell sorting strategy of Long-term hematopoietic stem cells (LT-HSCs), short-term hematopoietic stem cells (ST-HSCs), multipotent progenitors (MPPs), common myeloid progenitors (CMPs), common lymphoid progenitors (CLPs), granulocyte/monocyte progenitors (GMPs), megakaryocyte/erythroid progenitors (MEPs). Three independent experiments.

Data are represented as mean ± SD. ** $P < 0.01$, *** $P < 0.001$.

Supplementary Table 1. The primers used in the qRT-PCR analysis

Name	Primer (5'→3')
U6-F	GGAACGATACAGAGAAGATTAGC
U6-R	TGGAACGCTTCACGAATTTGCG
mmu-miR-221-3p	AGCTACATTGTCTGCTGGGTTTC
mmu-miR-181b-5p	AACATTCATTGCTGTCGGTGGGTT
mmu-miR-181d-5p	AACATTCATTGTTGTCGGTGGGT
mmu-miR-27a-5p	AGGGCTTAGCTGCTTGTGAGCA
mmu-miR-129-5p	CTTTTTGCGGTCTGGGCTTGC
mmu-miR-6538	CGCGGGCTCCGGGGCGGCG
mmu-miR-23a-5p	GGGGTTCCTGGGGATGGGATTT
mmu-miR-5100	TCGAATCCCAGCGGTGCCTCT
mmu-miR-222-3p	CTCAGTAGCCAGTGTAGATCC
mmu-miR-331-3p	CTAGGTATGGTCCCAGGGATCC
mmu-miR-877-5p	GTAGAGGAGATGGCGCAGGG
mmu-miR-3968	CGAATCCCACTCCAGACACCA
mmu-miR-219a-1-3p	TGATTGTCCAAACGCAATTCT
mmu-miR-3473f	CAAATAGGACTGGAGAGATG
mmu-miR-298-5p	GGCAGAGGAGGGCTGTTCTTCCC
mmu-miR-3963	TGTATCCCACTTCTGACAC
mmu-miR-34c-3p	AATCACTAACCACACAGCCAGG
mmu-miR-351-3p	GGTCAAGAGGCGCCTGGGAAC
mmu-miR-130b-5p	ACTCTTTCCCTGTTGCACTACT
mmu-miR-5099	TTAGATCGATGTGGTGCTCC
mmu-miR-709	GGAGGCAGAGGCAGGAGGA
mmu-miR-3473a	TGGAGAGATGGCTCAGCA
mmu-miR-3473b	GGGCTGGAGAGATGGCTCAG
mmu-miR-1931	ATGCAAGGGCTGGTGCGATGGC

mmu-miR-6240	CCAAAGCATCGCGAAGGCCCACGGCG
mmu-miR-296-3p	GAGGGTTGGGTGGAGGCTCTCC
mmu-miR-6238	TTATTAGTCAGTGGAGGAAATG
mmu-miR-3470a	TCACTTTGTAGACCAGGCTGG
mmu-miR-3470b	TCACTCTGTAGACCAGGCTGG
mmu-miR-690	AAAGGCTAGGCTCACAACCAAA
mmu-miR-1195	TGAGTTCGAGGCCAGCCTGCTCA
mmu-miR-196b-3p	TCGACAGCACGACACTGCCTTC
mmu-miR-221-5p	ACCTGGCATACAATGTAGATTTCTGT
mmu-miR-222-5p	TCAGTAGCCAGTGTAGATCCT
mmu-miR-223-5p	CGTGTATTTGACAAGCTGAGTTG
Gapdh-F	GTCTCCTCTGACTTCAACAGCG
Gapdh-R	ACCACCCTGTTGCTGTAGCCAA
Gbp2-F	TCACAGAGGCAGCAAAGGAG
Gbp2-R	TGCTGCATCATCAGCTCGAA

Supplementary Table 2. The oligonucleotides used in this study

Name	Sequence (5'→3')
Oligos-F for miR-221 overexpression	GATCCGCCAGCAGACAATGTAGCTCTCCTGCTACCCTGACCCAGTAGCCCAAGAGCTACATTGTCTGCTGGCTTTTTTG
Oligos-R for miR-221 overexpression	AATTCAAAAAAGCCAGCAGACAATGTAGCTCTTGGGCTACTGGGTCAGGGTAGCAGGAGAGCTACATTGTCTGCTGGCG
Gbp2-shRNA1-F	CCGGGATGTTGTTGAAACACTTCTACTCGAGTAGAAGTGTTTCAACAACATCTTTTT
Gbp2-shRNA1-R	GATCAAAAAGATGTTGTTGAAACACTTCTACTCGAGTAGAAGTGTTTCAACAACATC
Gbp2-shRNA2-F	CCGGGCGACTGTGCATCAGGAAATTCTCGAGAATTTCCTGATGCACAGTCGCTTTTT
Gbp2-shRNA2-R	GATCAAAAAGCGACTGTGCATCAGGAAATTCTCGAGAATTTCCTGATGCACAGTCGC
miRNA negative control (miRNA NC)	UUCUCCGAACGUGUCACGUTT
miR-221 mimic	UAACACUGUCUGGUAAAGAUGG

Figure S1

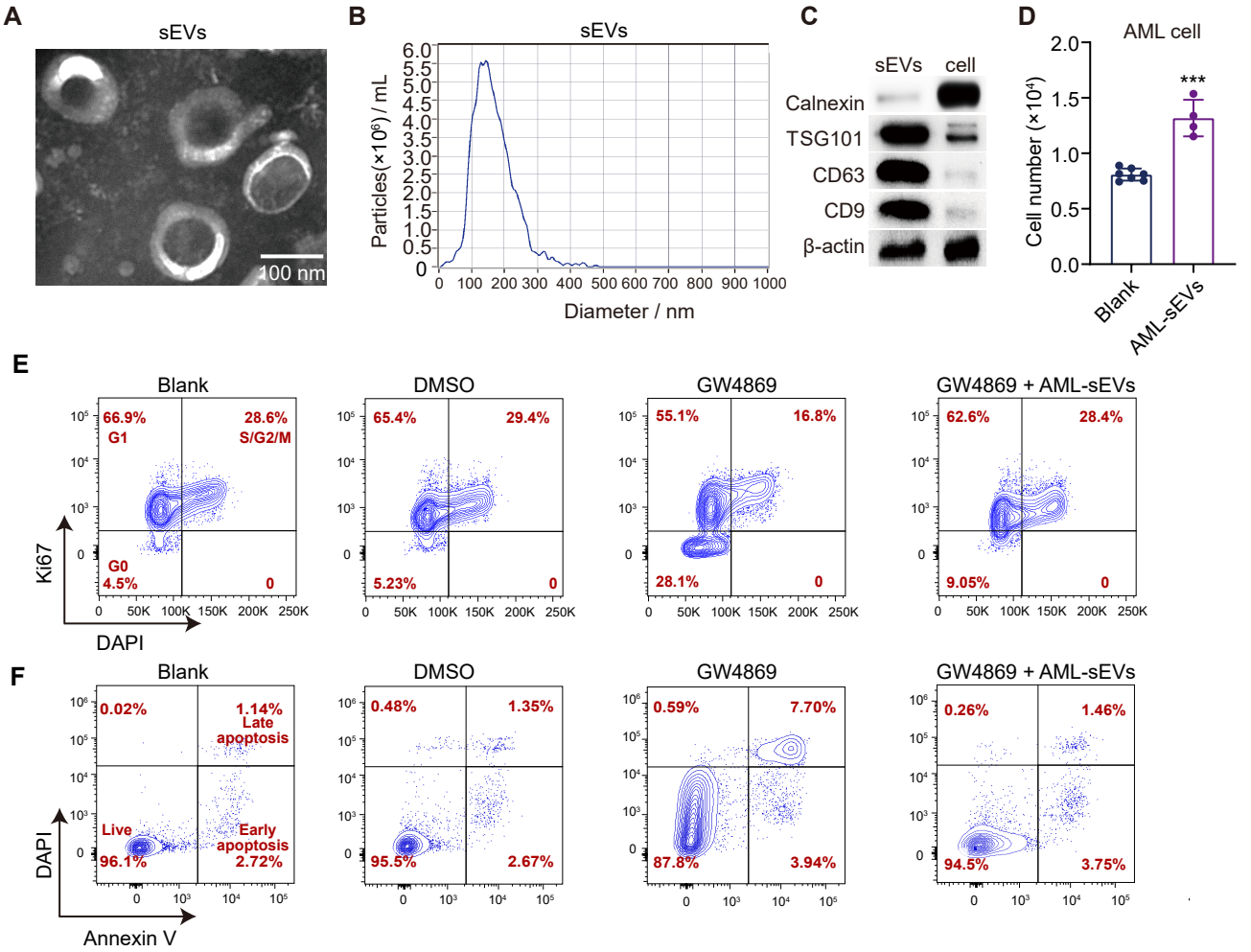
A
sEVs
100 nm
B
sEVs
Particles(×10⁶) / mL
Diameter / nm
C
sEVs
cell
Calnexin
TSG101
CD63
CD9
β-actin
D
AML cell
Cell number (×10⁴)
***
Blank
AML-sEVs
E
Blank
DMSO
GW4869
GW4869 + AML-sEVs
66.9%
G1
28.6%
S/G2/M
G0
4.5%
0
65.4%
29.4%
5.23%
55.1%
16.8%
28.1%
62.6%
28.4%
9.05%
Ki67
DAPI
F
Blank
DMSO
GW4869
GW4869 + AML-sEVs
0.02%
1.14%
Late
apoptosis
Live
96.1%
Early
apoptosis
2.72%
0.48%
1.35%
95.5%
2.67%
0.59%
7.70%
87.8%
3.94%
0.26%
1.46%
94.5%
3.75%
DAPI
Annexin V

Figure S2

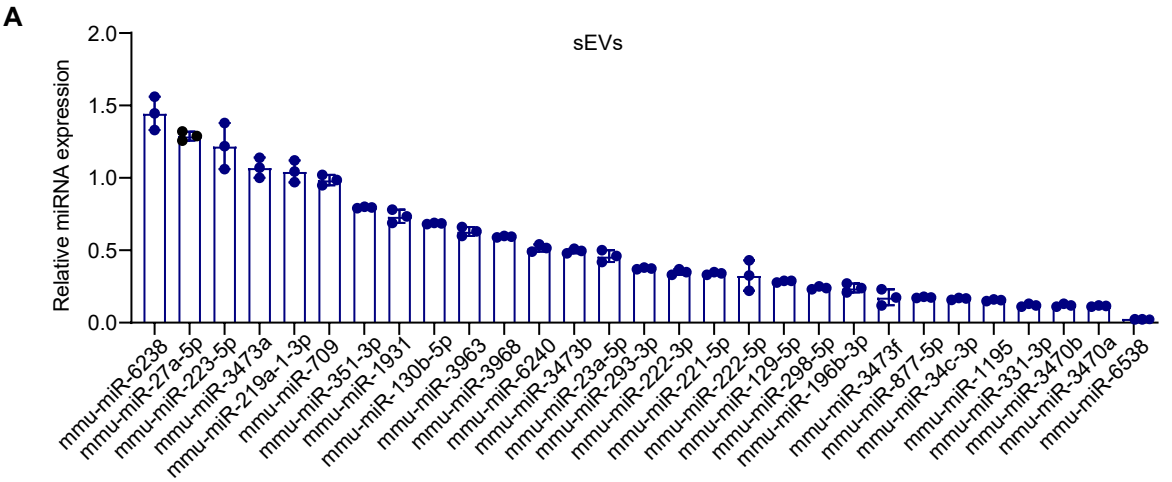

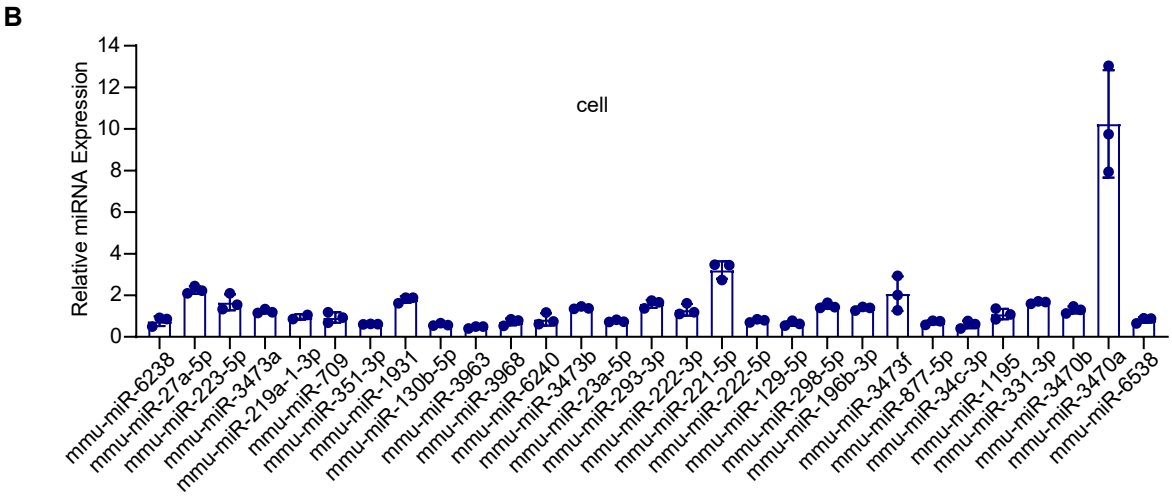

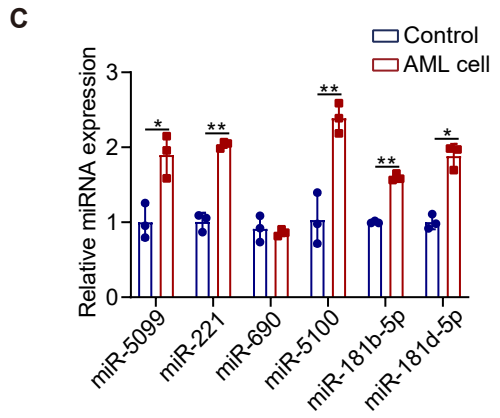

D

miR-221

seed sequence

Homo sapiens	AGCUACAUUGUCUGCUGGGUUUC
Mus musculus	AGCUACAUUGUCUGCUGGGUUUC
Rattus norvegicus	AGCUACAUUGUCUGCUGGGUUUC
Macaca mulatta	AGCUACAUUGUCUGCUGGGUUUC
Sus scrofa	AGCUACAUUGUCUGCUGGGUUUC
Gallus gallus	AGCUACAUUGUCUGCUGGGUUUC
Danio rerio	AGCUACAUUGUCUGCUGGGUUUC

Figure S3

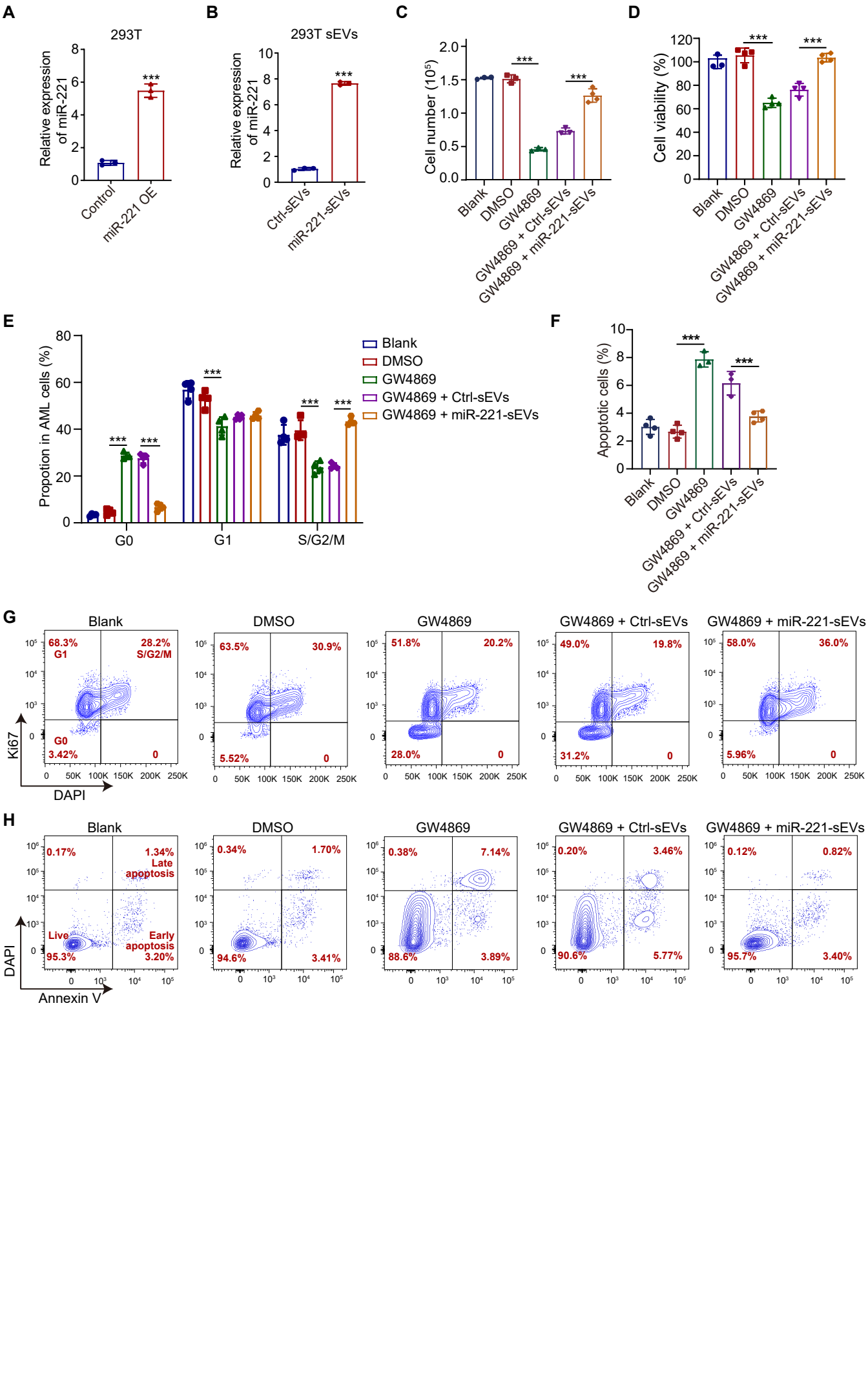
A
293T
Relative expression of miR-221
Control
miR-221 OE
B
293T sEVs
Relative expression of miR-221
Ctrl-sEVs
miR-221-sEVs
C
Cell number (10^5)
Blank
DMSO
GW4869
GW4869 + Ctrl-sEVs
GW4869 + miR-221-sEVs
D
Cell viability (%)
E
Propotion in AML cells (%)
G0
G1
S/G2/M
F
Apoptotic cells (%)
G
Blank
DMSO
GW4869
GW4869 + Ctrl-sEVs
GW4869 + miR-221-sEVs
68.3%
G1
28.2%
S/G2/M
G0
3.42%
0
63.5%
30.9%
5.52%
51.8%
20.2%
28.0%
49.0%
19.8%
31.2%
58.0%
36.0%
5.96%
Ki67
DAPI
H
0.17%
1.34%
Late apoptosis
Live
95.3%
Early apoptosis
3.20%
0.34%
1.70%
94.6%
3.41%
0.38%
7.14%
88.6%
3.89%
0.20%
3.46%
90.6%
5.77%
0.12%
0.82%
95.7%
3.40%
DAPI
Annexin V

Figure S4

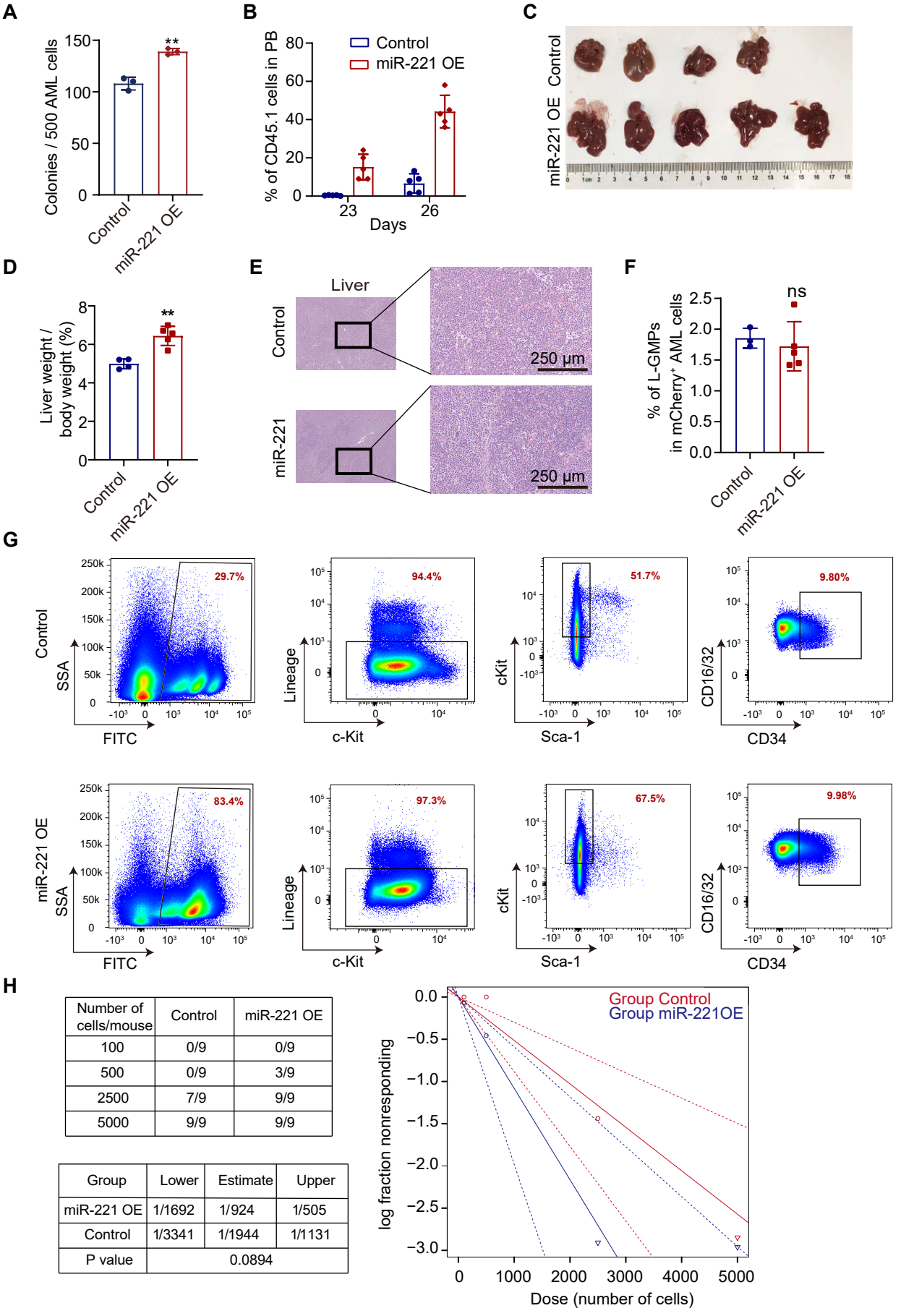

H

Number of cells/mouse	Control	miR-221 OE
100	0/9	0/9
500	0/9	3/9
2500	7/9	9/9
5000	9/9	9/9

Group	Lower	Estimate	Upper
miR-221 OE	1/1692	1/924	1/505
Control	1/3341	1/1944	1/1131
P value	0.0894		

Figure S5

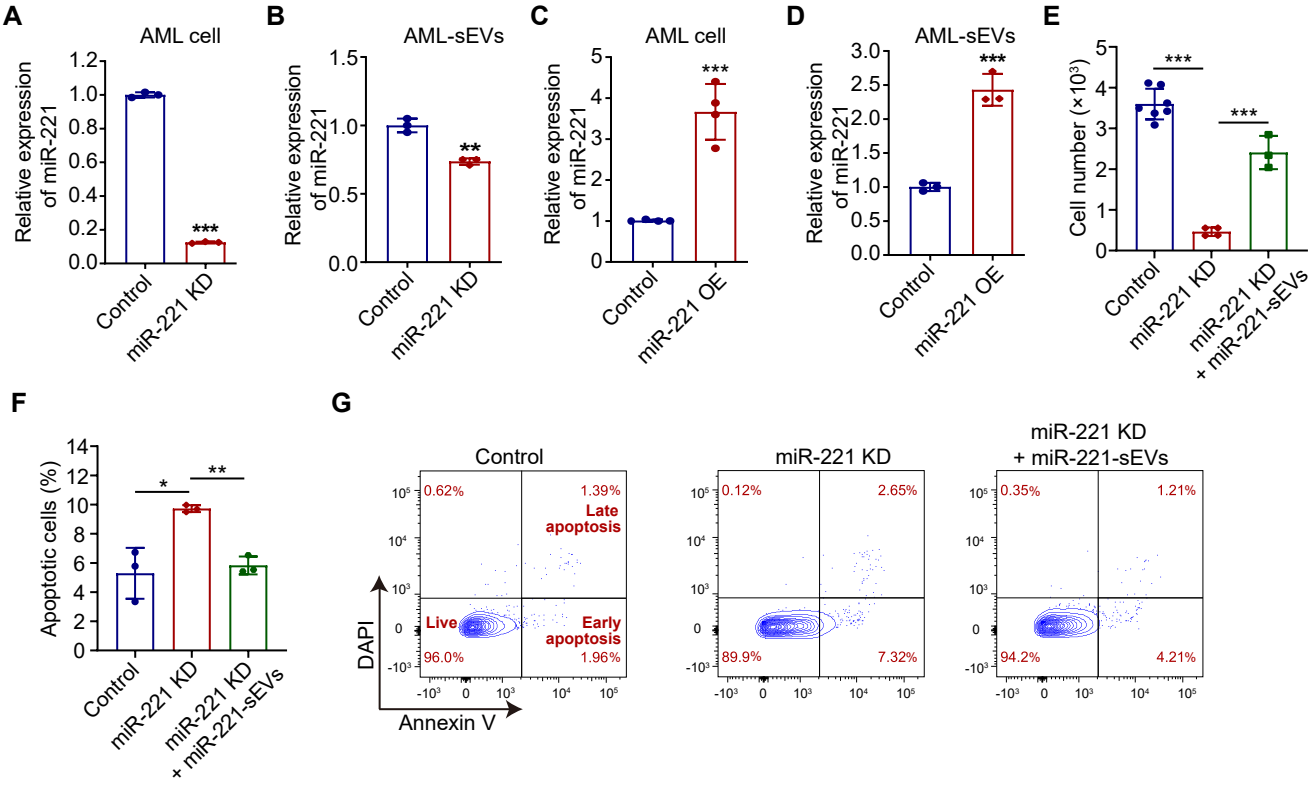
A
AML cell
Relative expression of miR-221
Control
miR-221 KD
B
AML-sEVs
Relative expression of miR-221
Control
miR-221 KD
C
AML cell
Relative expression of miR-221
Control
miR-221 OE
D
AML-sEVs
Relative expression of miR-221
Control
miR-221 OE
E
Cell number (×10³)
Control
miR-221 KD
miR-221 KD + miR-221-sEVs
F
Apoptotic cells (%)
Control
miR-221 KD
miR-221 KD + miR-221-sEVs
G
Control
miR-221 KD
miR-221 KD + miR-221-sEVs
0.62%
1.39%
Late apoptosis
Live
Early apoptosis
96.0%
1.96%
0.12%
2.65%
89.9%
7.32%
0.35%
1.21%
94.2%
4.21%
DAPI
Annexin V

Figure S6

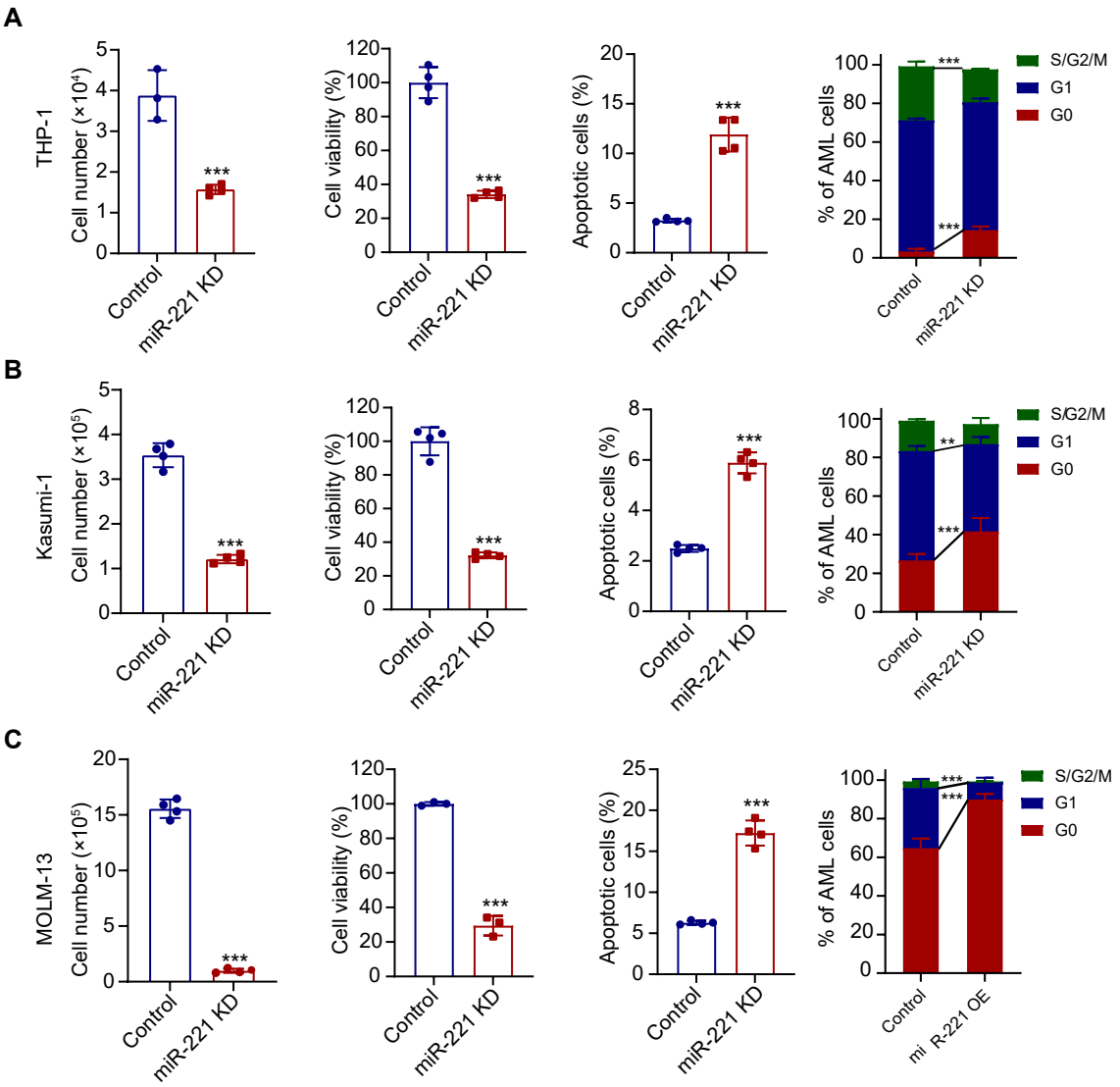
A
THP-1
Cell number (×10⁴)
Cell viability (%)
Apoptotic cells (%)
% of AML cells
S/G2/M
G1
G0
Control
miR-221 KD
B
Kasumi-1
Cell number (×10⁵)
C
MOLM-13
miR-221 OE

Figure S7

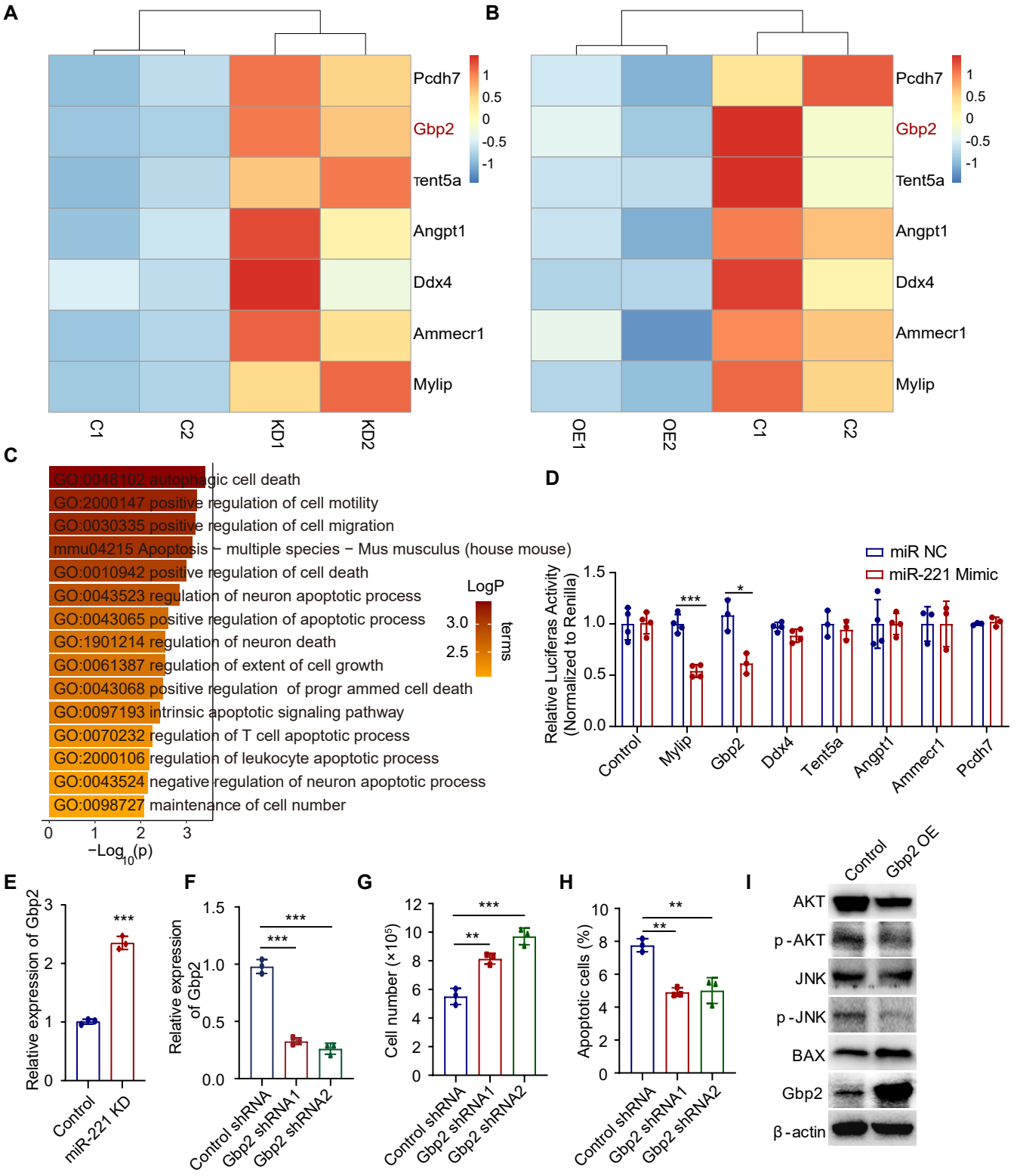
A
Pcdh7
Gbp2
Tent5a
Angpt1
Ddx4
Ammecr1
Mylip
C1
C2
KD1
KD2
1
0.5
0
-0.5
-1
B
Pcdh7
Gbp2
Tent5a
Angpt1
Ddx4
Ammecr1
Mylip
OE1
OE2
C1
C2
C
GO:0048102 autophagic cell death
GO:2000147 positive regulation of cell motility
GO:0030335 positive regulation of cell migration
mmu04215 Apoptosis − multiple species − Mus musculus (house mouse)
GO:0010942 positive regulation of cell death
GO:0043523 regulation of neuron apoptotic process
GO:0043065 positive regulation of apoptotic process
GO:1901214 regulation of neuron death
GO:0061387 regulation of extent of cell growth
GO:0043068 positive regulation of progr ammed cell death
GO:0097193 intrinsic apoptotic signaling pathway
GO:0070232 regulation of T cell apoptotic process
GO:2000106 regulation of leukocyte apoptotic process
GO:0043524 negative regulation of neuron apoptotic process
GO:0098727 maintenance of cell number
LogP
3.0
2.5
terms
0
1
2
3
−Log10(p)
D
miR NC
miR-221 Mimic
Relative Luciferas Activity (Normalized to Renilla)
1.5
1.0
0.5
0.0
***
*
Control
Mylip
Gbp2
Ddx4
Tent5a
Angpt1
Ammecr1
Pcdh7
E
Relative expression of Gbp2
3
2
1
0
***
Control
miR-221 KD
F
Relative expression of Gbp2
1.5
1.0
0.5
0.0
***
***
Control shRNA
Gbp2 shRNA1
Gbp2 shRNA2
G
Cell number (×10⁵)
12
10
8
6
4
2
0
***
**
Control shRNA
Gbp2 shRNA1
Gbp2 shRNA2
H
Apoptotic cells (%)
10
8
6
4
2
0
**
**
Control shRNA
Gbp2 shRNA1
Gbp2 shRNA2
I
Control
Gbp2 OE
AKT
p-AKT
JNK
p-JNK
BAX
Gbp2
β-actin

Figure S8

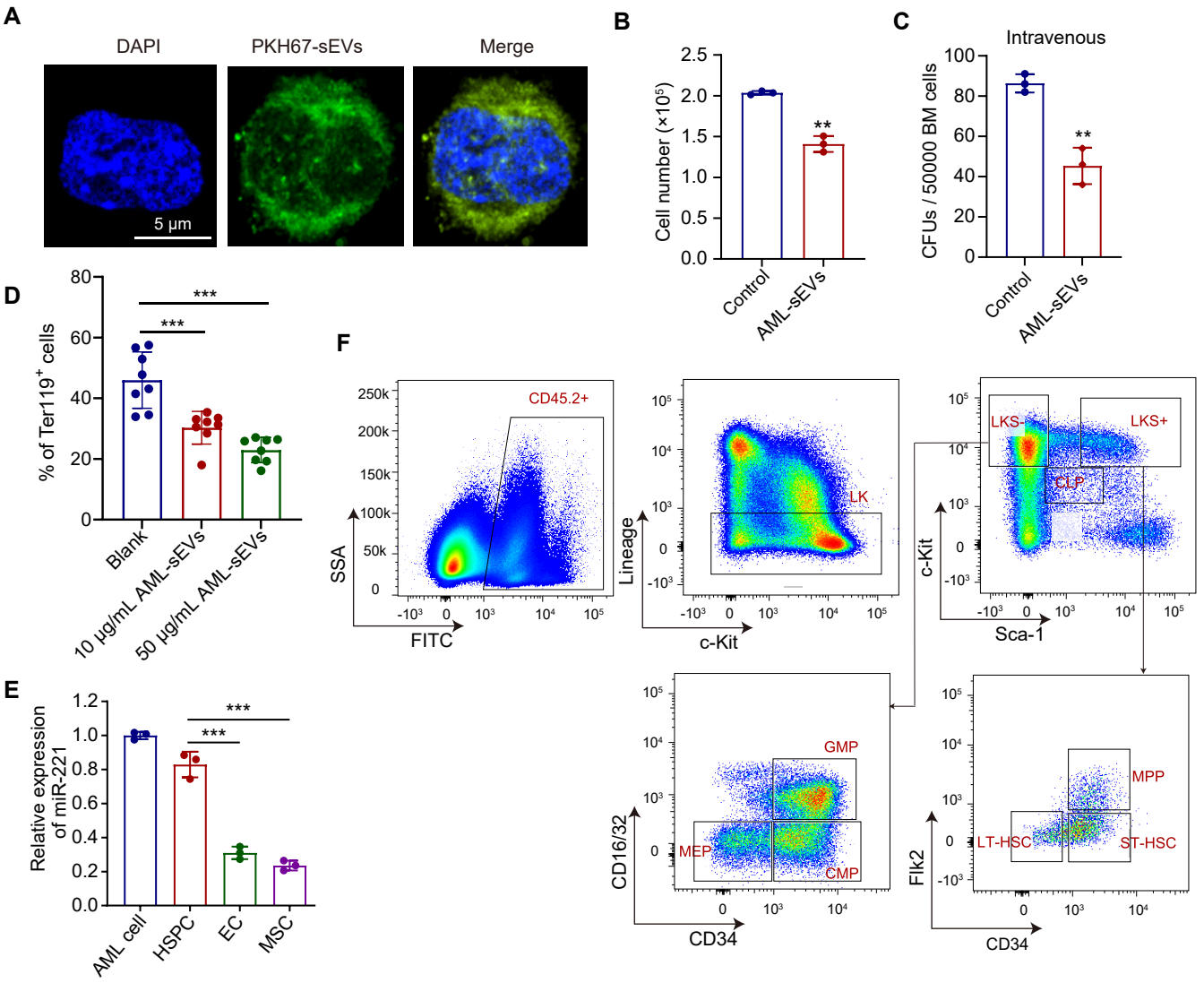
A
DAPI
PKH67-sEVs
Merge
5 μm
B
Cell number (×10⁵)
Control
AML-sEVs
C
Intravenous
CFUs / 50000 BM cells
Control
AML-sEVs
D
% of Ter119⁺ cells
Blank
10 μg/mL AML-sEVs
50 μg/mL AML-sEVs
E
Relative expression of miR-221
AML cell
HSPC
EC
MSC
F
CD45.2+
SSA
FITC
Lineage
LK
c-Kit
LKS-
LKS+
CLP
Sca-1
GMP
MEP
CMP
CD16/32
CD34
MPP
LT-HSC
ST-HSC
Flk2
CD34